

LA-UR-21-21115

Approved for public release; distribution is unlimited.

Title: Exploration of the Solar System using Gamma-Ray and Neutron Spectrometers

Author(s): Nowicki, Suzanne Florence

Intended for: Science on Tap

Issued: 2021-02-08

Disclaimer:

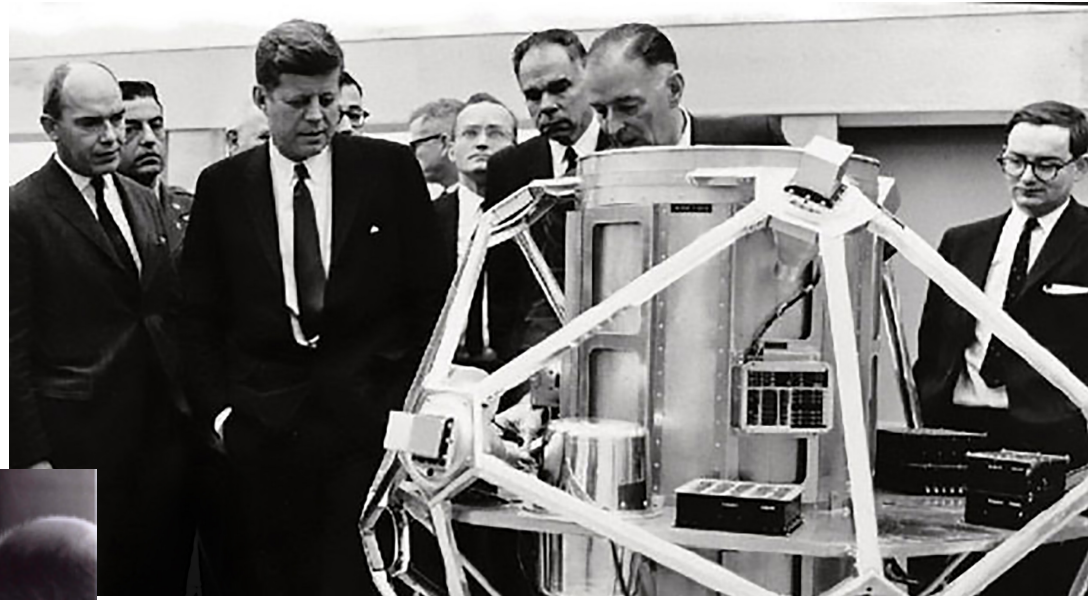
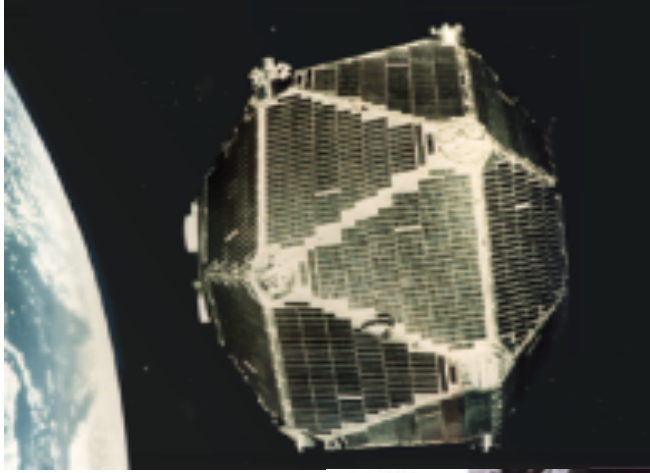
Los Alamos National Laboratory, an affirmative action/equal opportunity employer, is operated by Triad National Security, LLC for the National Nuclear Security Administration of U.S. Department of Energy under contract 89233218CNA000001. By approving this article, the publisher recognizes that the U.S. Government retains nonexclusive, royalty-free license to publish or reproduce the published form of this contribution, or to allow others to do so, for U.S. Government purposes. Los Alamos National Laboratory requests that the publisher identify this article as work performed under the auspices of the U.S. Department of Energy. Los Alamos National Laboratory strongly supports academic freedom and a researcher's right to publish; as an institution, however, the Laboratory does not endorse the viewpoint of a publication or guarantee its technical correctness.

Exploration of the Solar System using Gamma-Ray and Neutron Spectrometers

Suzanne Nowicki

Space Science and Applications Group

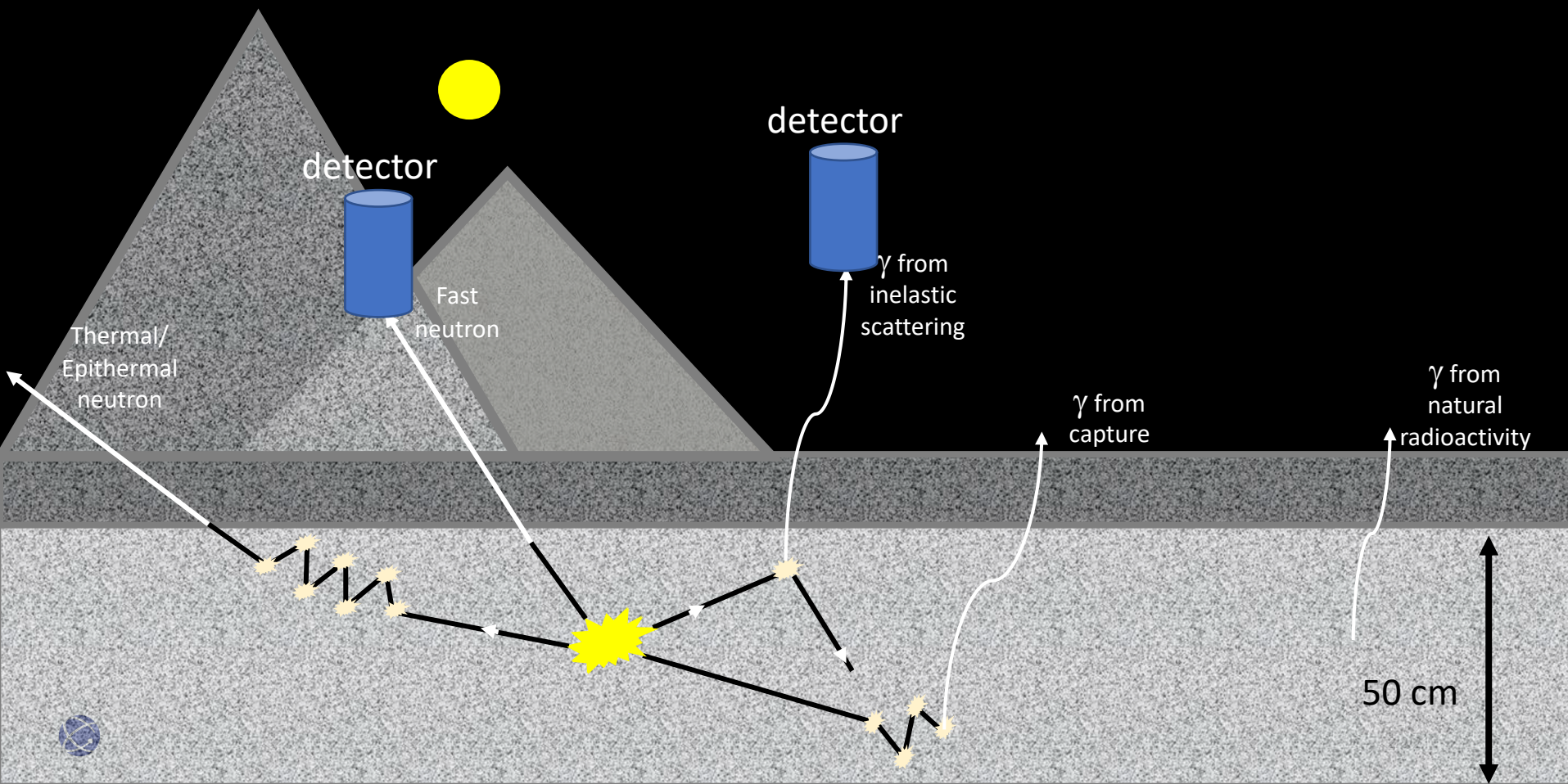
Feb. 8 2021



Project Vela, a program to develop satellite instruments that could detect nuclear detonations in the upper atmosphere and outer space.

On the morning of October 17, 1963, an Atlas-Agena-D rocket was launched from Cape Canaveral Air Force Station in Florida carrying the twin satellites Vela 1A and Vela 1B.





Mars Odyssey Gamma-Ray Spectrometer

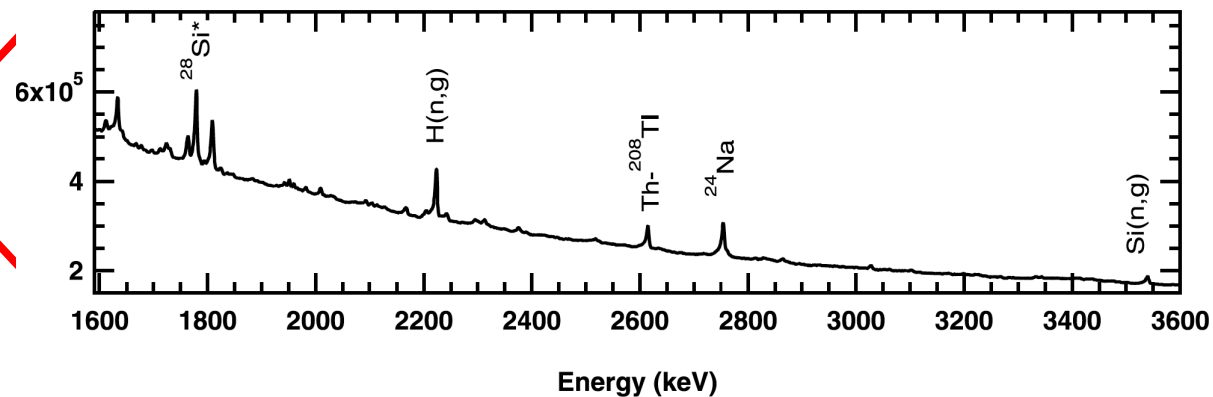
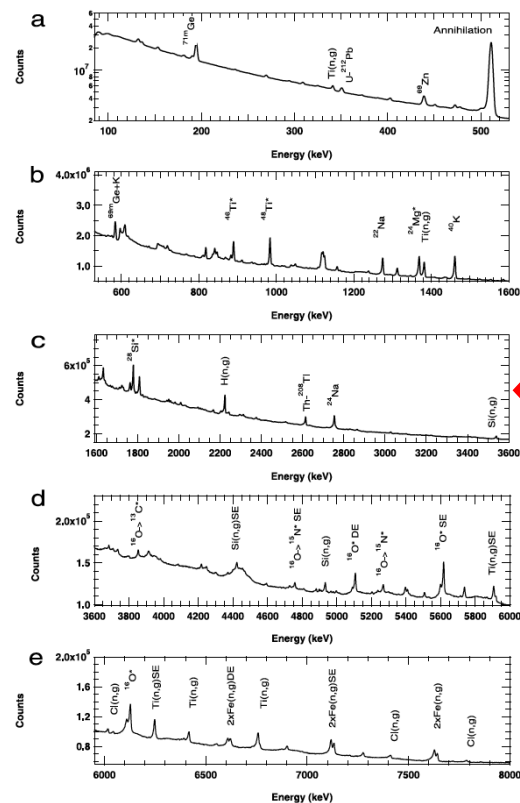
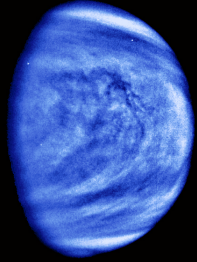
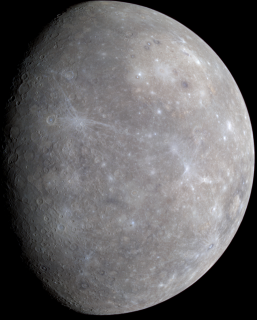


Figure 2. Details of the Mars spectrum shown in Figure 1. Some prominent gamma ray peaks are labeled in each plot. Neutron capture gamma rays are indicated with (n, γ). A nuclide with an asterisk after it indicates that the gamma ray is from an excited level of that nucleus that can be made by several processes. (a) Spectrum from 100 to 530 keV. (b) Spectrum from 530 to 1600 keV. (c) Spectrum from 1600 to 3600 keV. (d) Spectrum from 3600 to 6000 keV. (e) Spectrum from 5950 to 9000 keV. Single-escape and double-escape peaks are labeled with SE and DE, respectively.



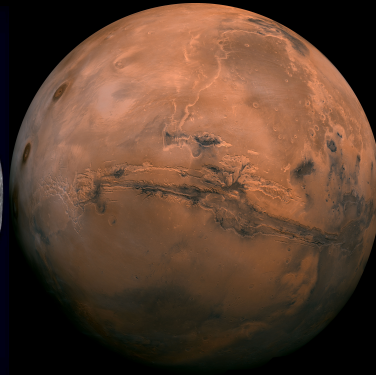
Venus



Mercury



Moon



Mars



Vesta

Eros



Ceres

credit: NASA/ESA

2004–2015

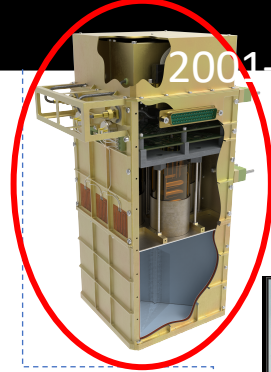


Gamma-Ray Spectrometer (GRS)

1971–1972



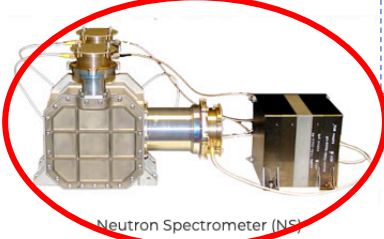
2009–
present



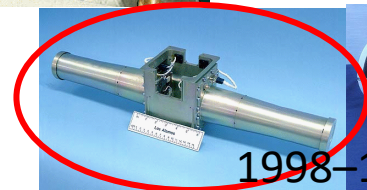
2001–present



2007–2018



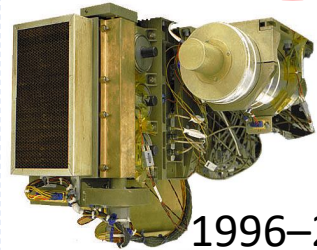
Neutron Spectrometer (NS)



1998–1999



2011–
present



1996–2001

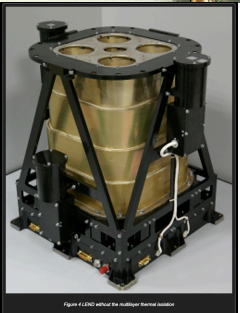


Gamma-Ray Spectrometer (GRS)

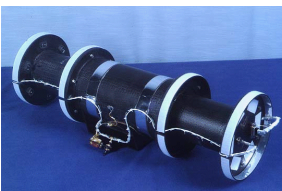
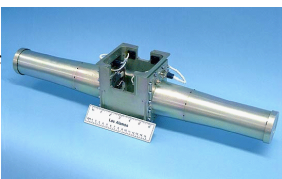
MESSENGER GRS and NS: 5 x 5 cm cylindrical **HPGe**. FWHM of 3.5 keV at 1332 keV. Miniature Stirling-cycle cooler, itself cooled via a large passive radiator. **Borated plastic** scintillator ACS.

2 **^6Li glass** scintillators on the ends separated by a beveled cube of neutron-absorbing, **borated plastic** scintillator with PMTs.

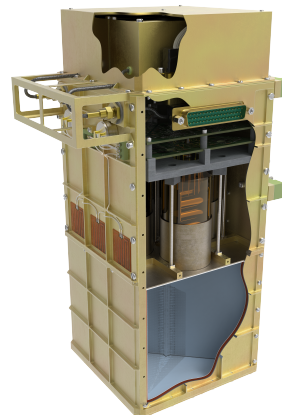
Apollo: **NaI(Tl)** 76 x 76 mm and **plastic** ACS. Mounted on 7.6 m long boom. Res. is 8% FWHM at 662 keV



LRO LEND: 3 **^3He** tubes covered with Cd. 4 **^3He** tubes. Collimator. **Stilbene** crystal, surrounded by a **plastic** scintillator ACS.



Lunar Prospector NS and GRS: Two 5 x 20 cm **He-3** tubes. One counter is covered with a 0.75 mm thick **Cd** shield. **BGO** with **B-loaded plastic** ACS.



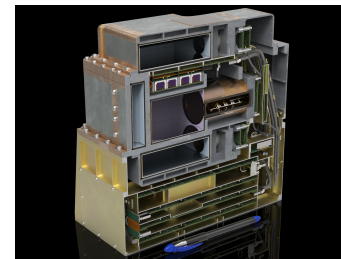
four prism-shaped quadrants of segmented block of **borated plastic** scintillator. 3.8 cm diameter. 0.69 mm **Cd**.



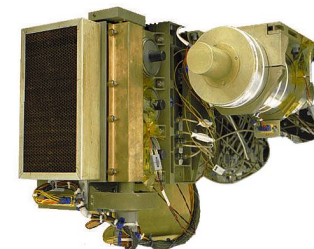
Passively cooled 6.7 x 6.7 cm cylindrical **HPGe**. FWHM of 2.8 keV at 1332 keV.



Mars Science Lab (Curiosity rover) Dynamic Albedo of neutrons: 14 MeV PNG and 2 neutron **He-3** tubes, one covered with **Cd**.

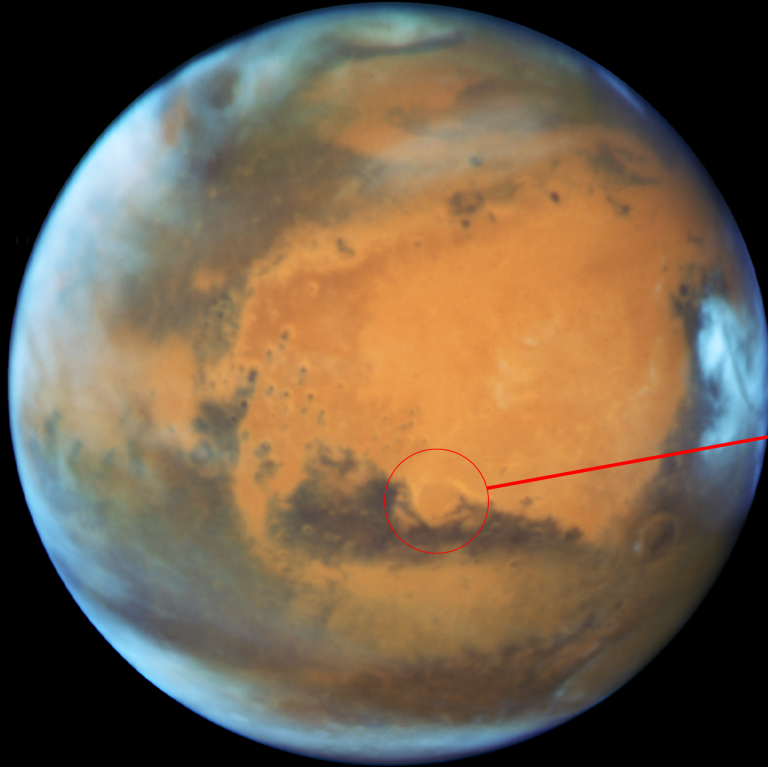


DAWN GRS: 4 by 4 **CZT** array. **BGO** surrounded by **plastic** scintillators. **^6Li -loaded glass** plate, optically coupled to a Gd-wrapped block of **B-loaded plastic** and readout by PMT.

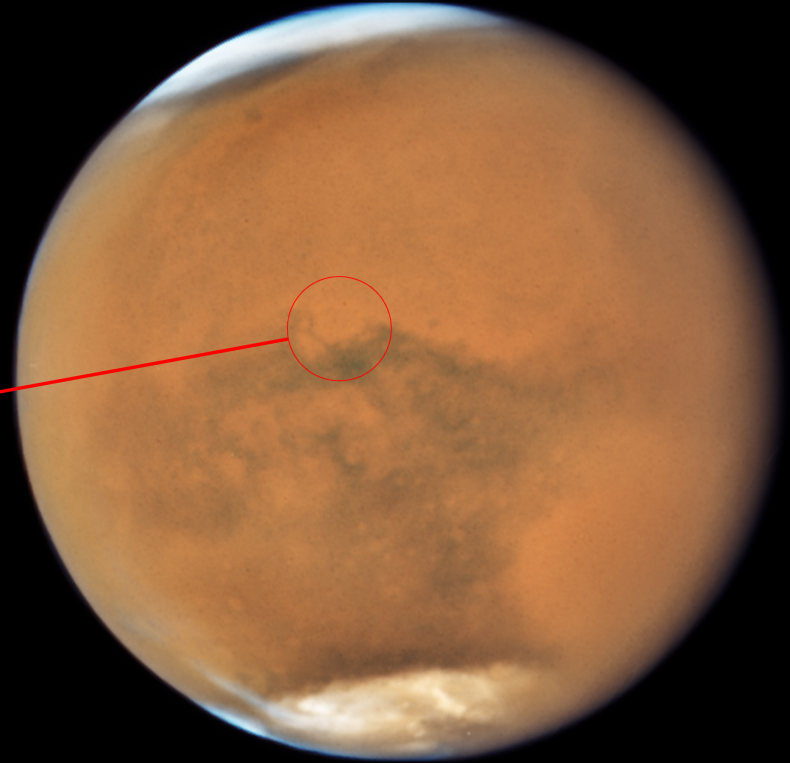


NEAR Shoemaker GRS: **NaI(Tl)** 2.5 x 7.5 cm with 8.5% FWHM at 662 keV. Shield detector is **BGO** 8.9 x 14 cm with 15% FWHM at 662 keV.

Mars Opposition

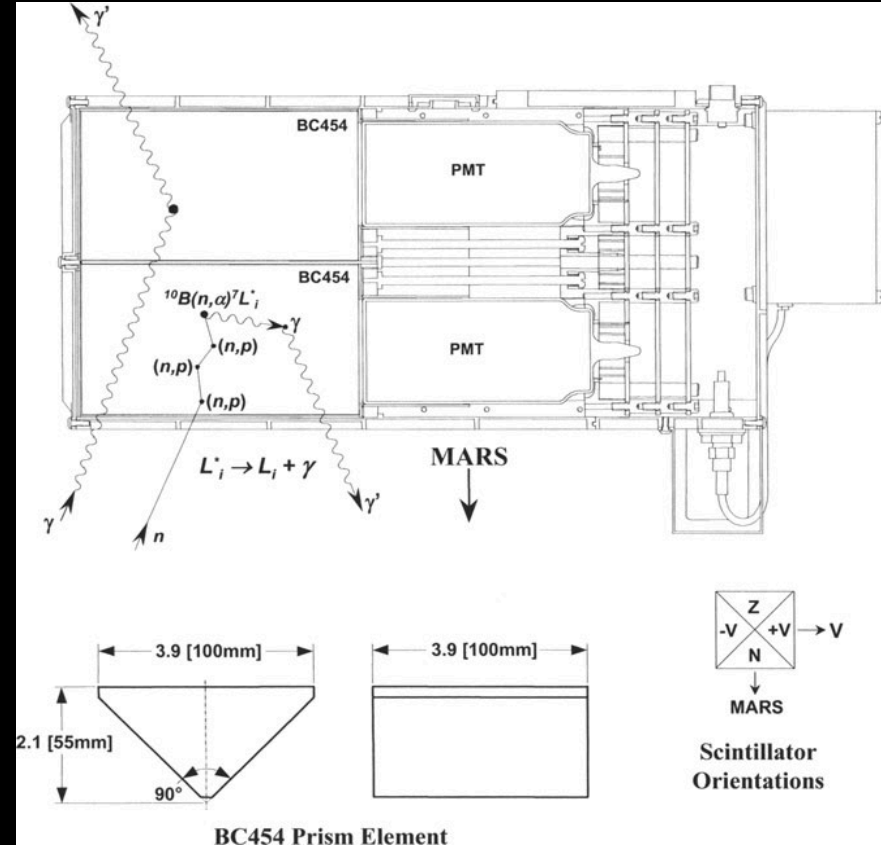


2016

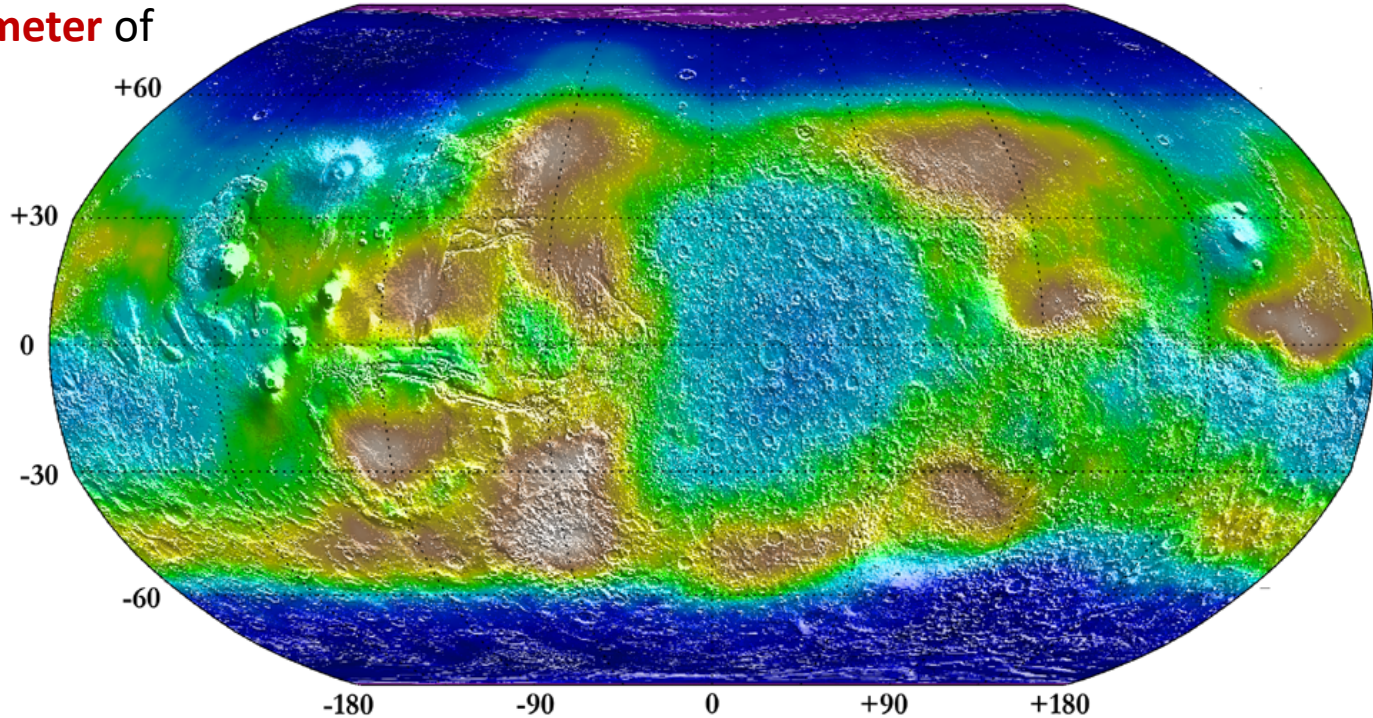
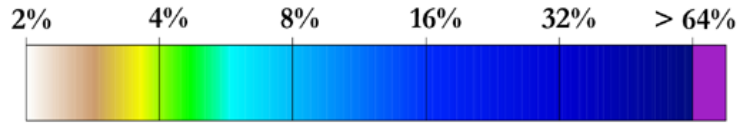


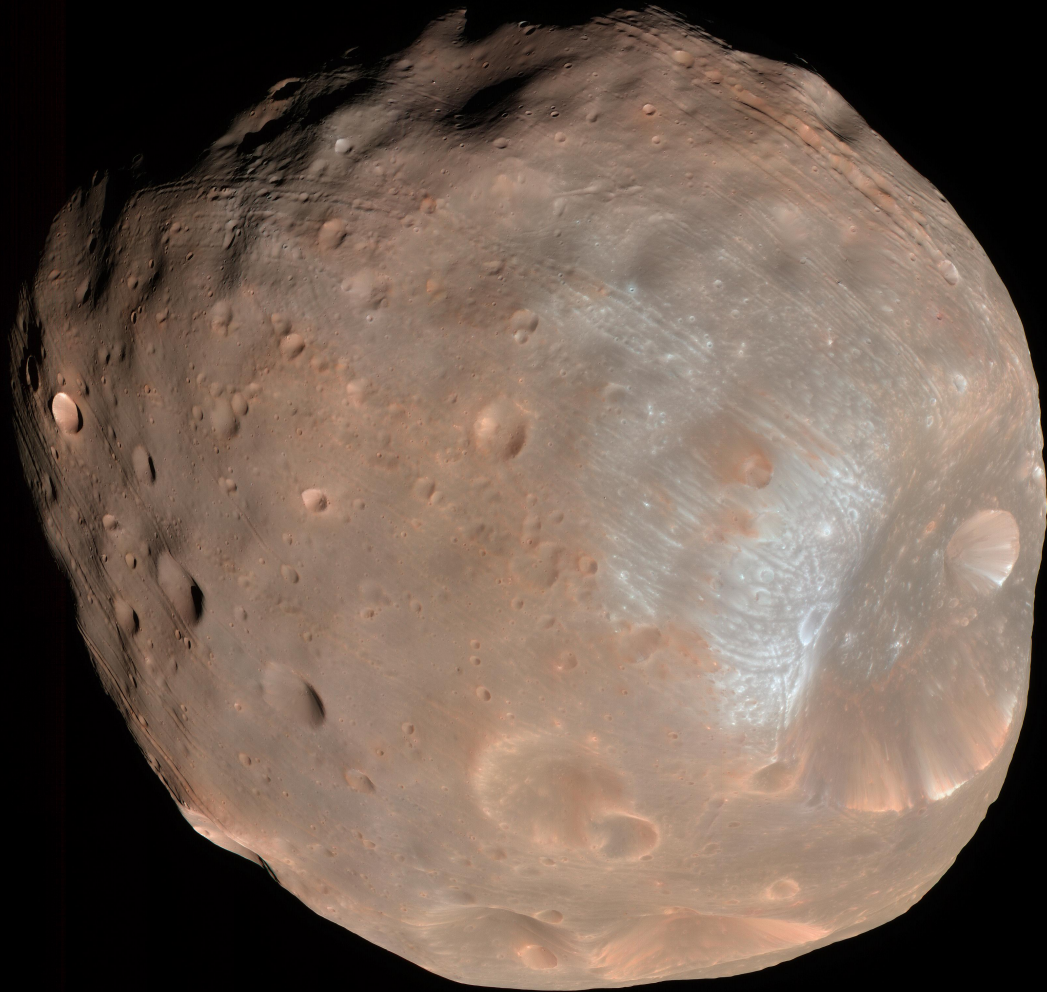
2018

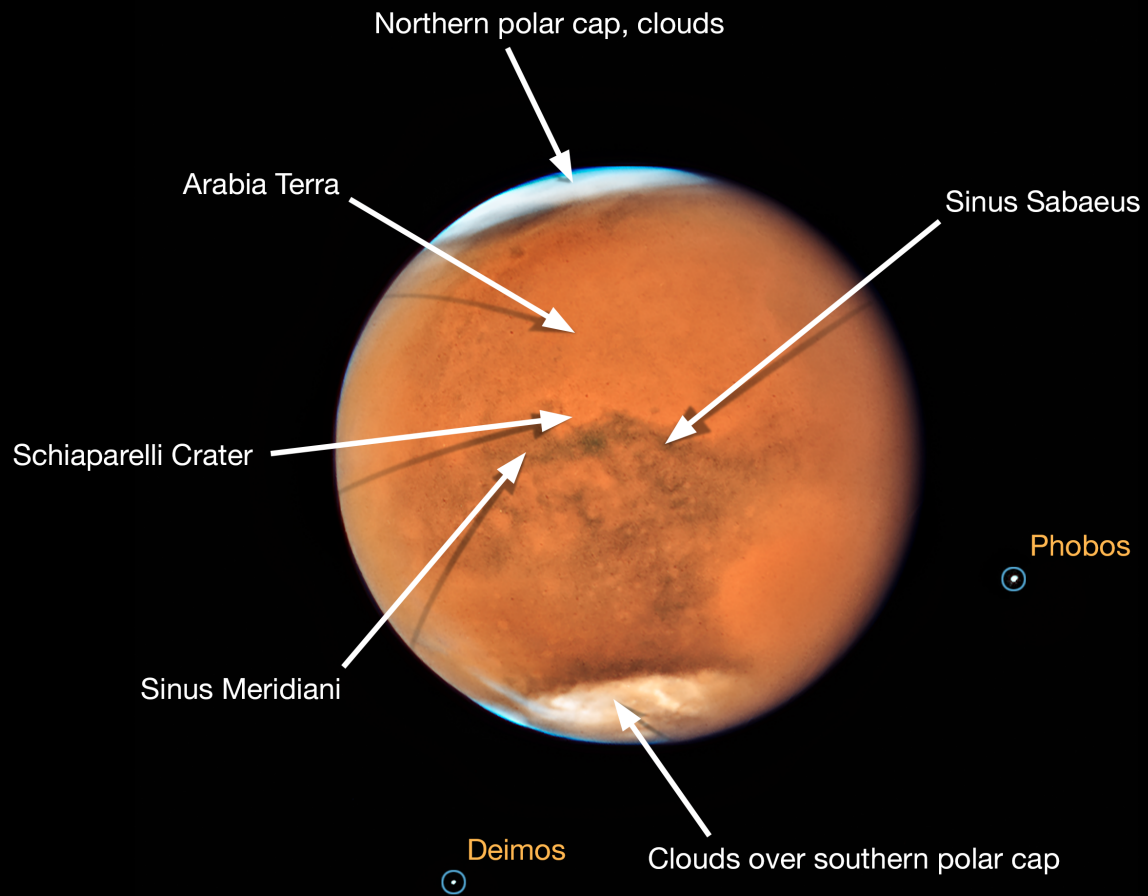
A detailed view of the internal components of the LISA Pathfinder spacecraft. The structure is primarily gold-colored, with a central test mass suspended by thin fibers. Various sensors, actuators, and wiring are visible, including a green circuit board and a blue component at the bottom. A blue pen is placed at the bottom for scale.



Lower-Limit of Water Mass Fraction on Mars

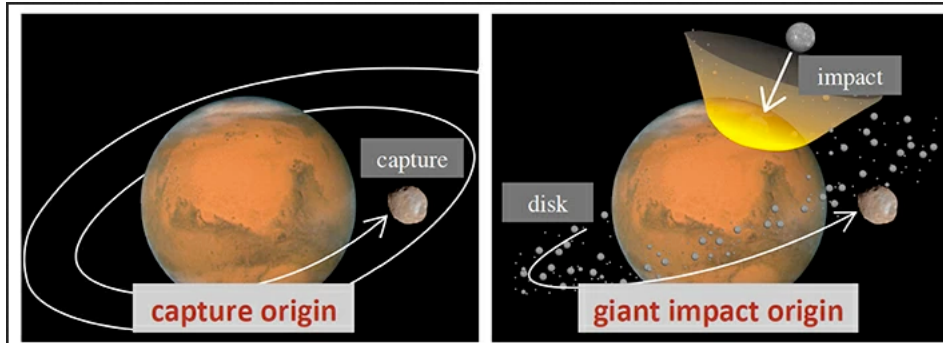






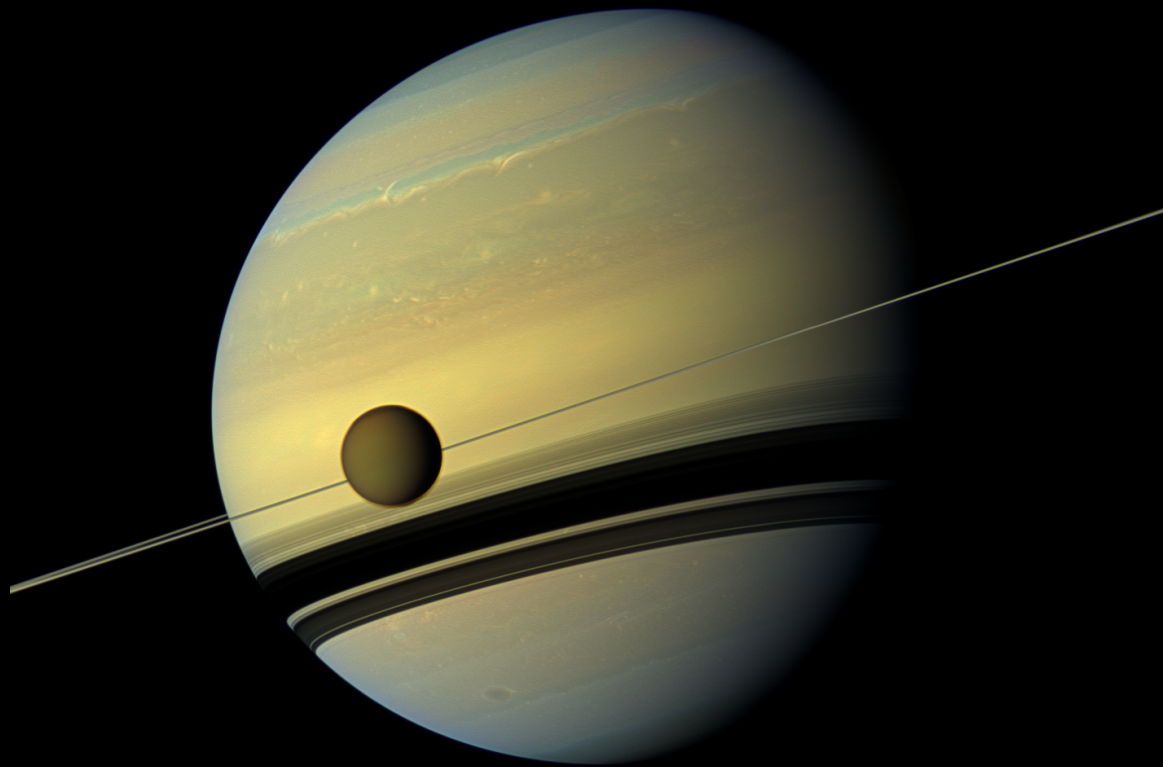
Origin of Martian Moons are not known. There are two leading hypotheses:

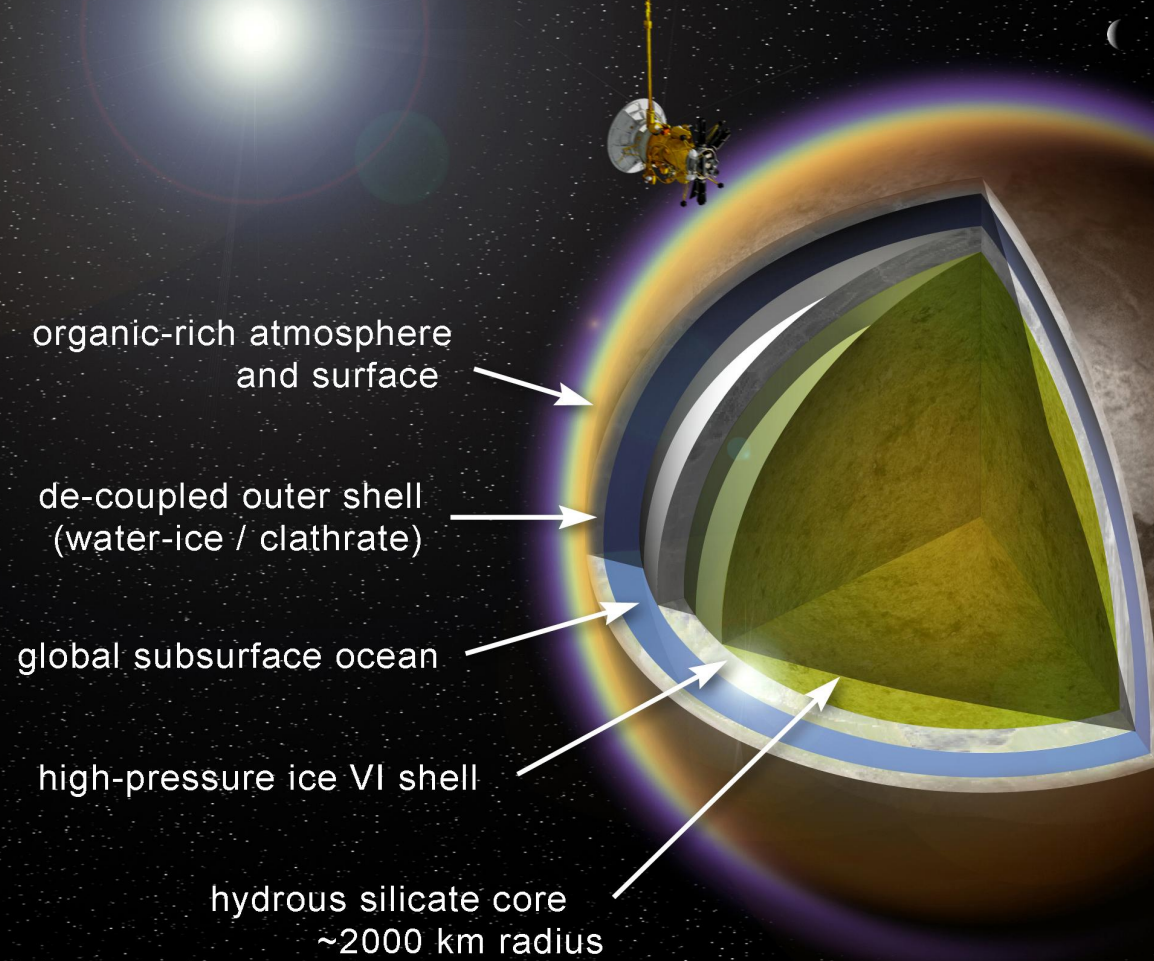
- 1) Captured primordial asteroid ?
- 2) Giant impact?



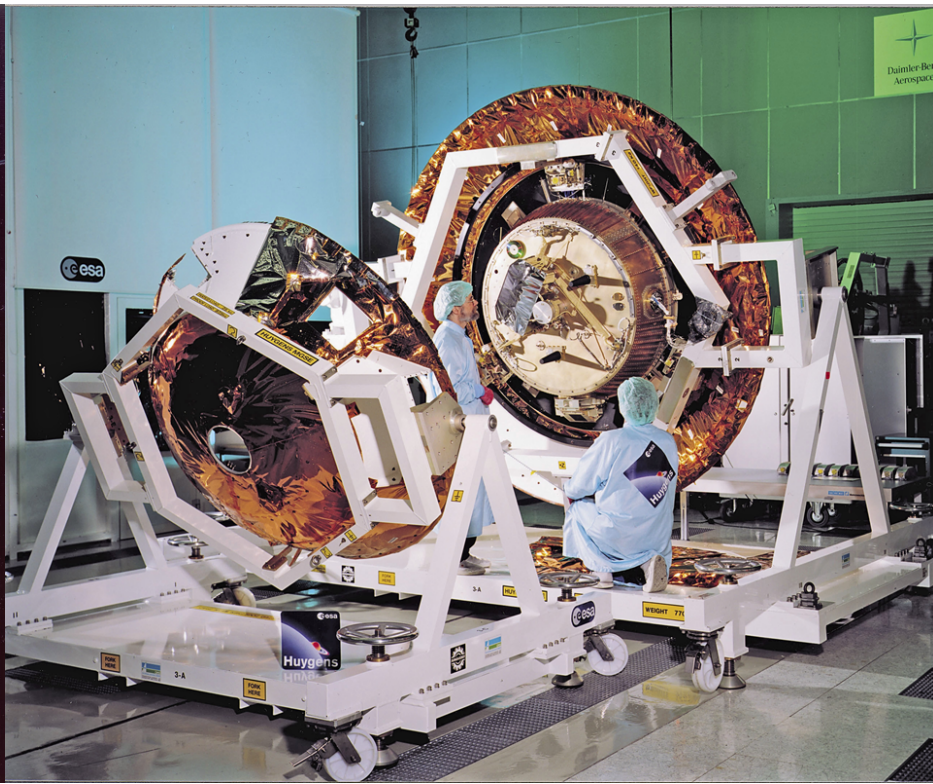
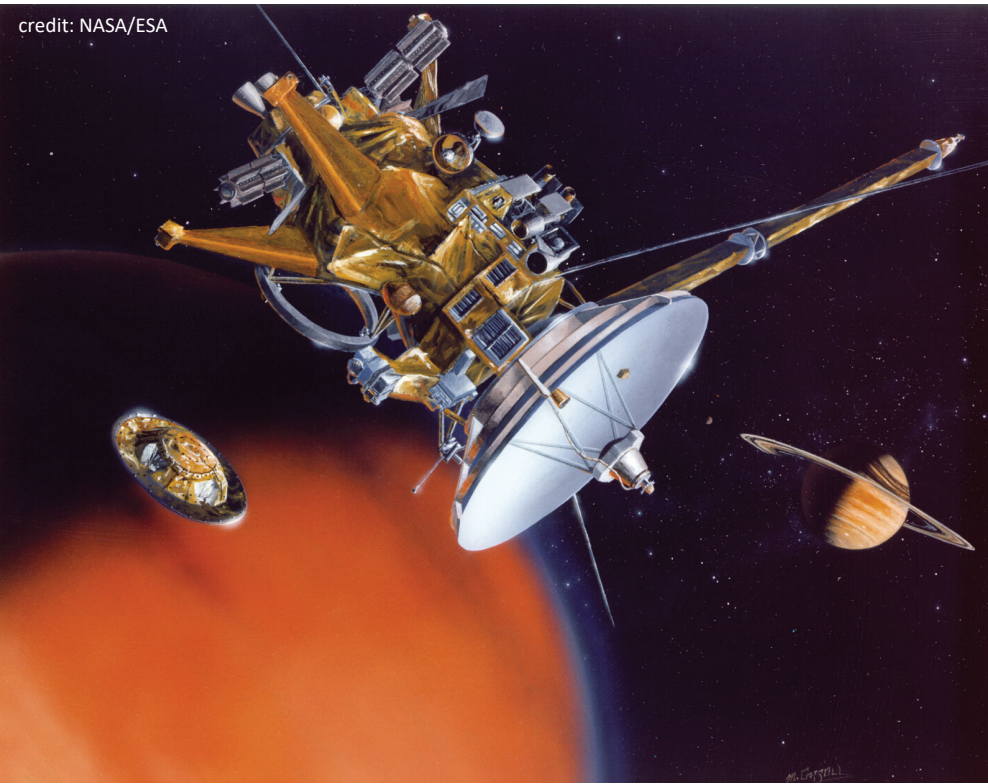
MASCOT

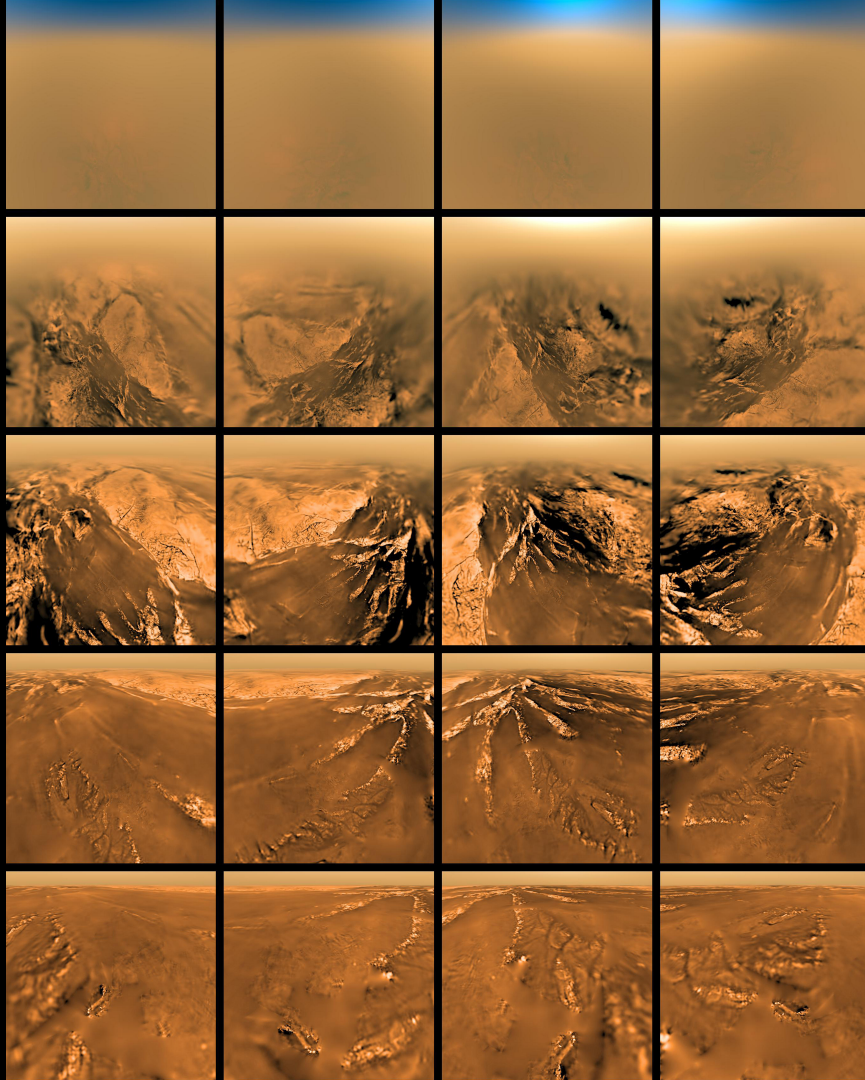


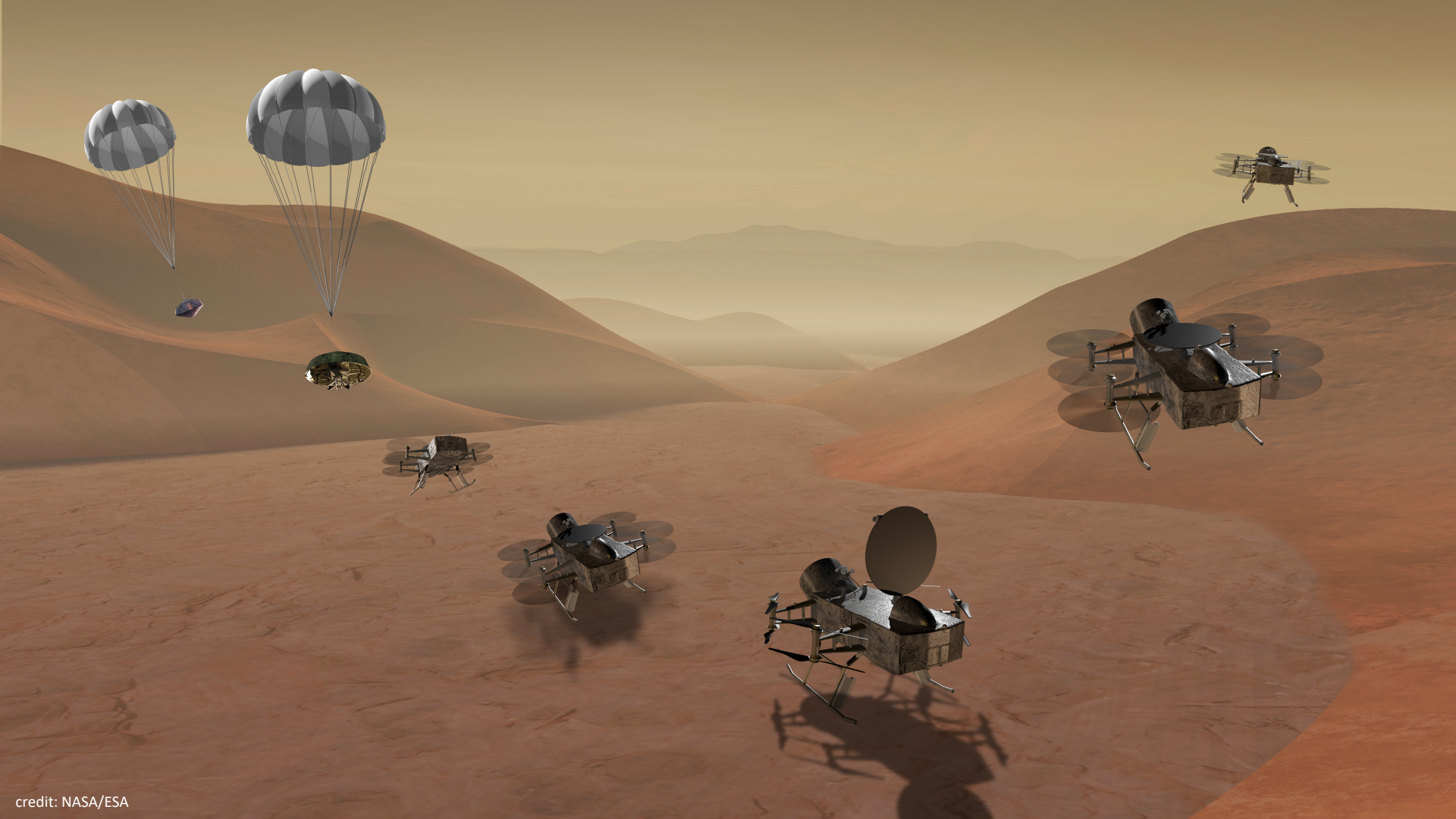


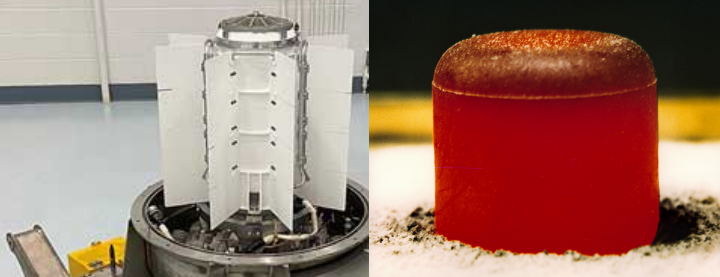


credit: NASA/ESA

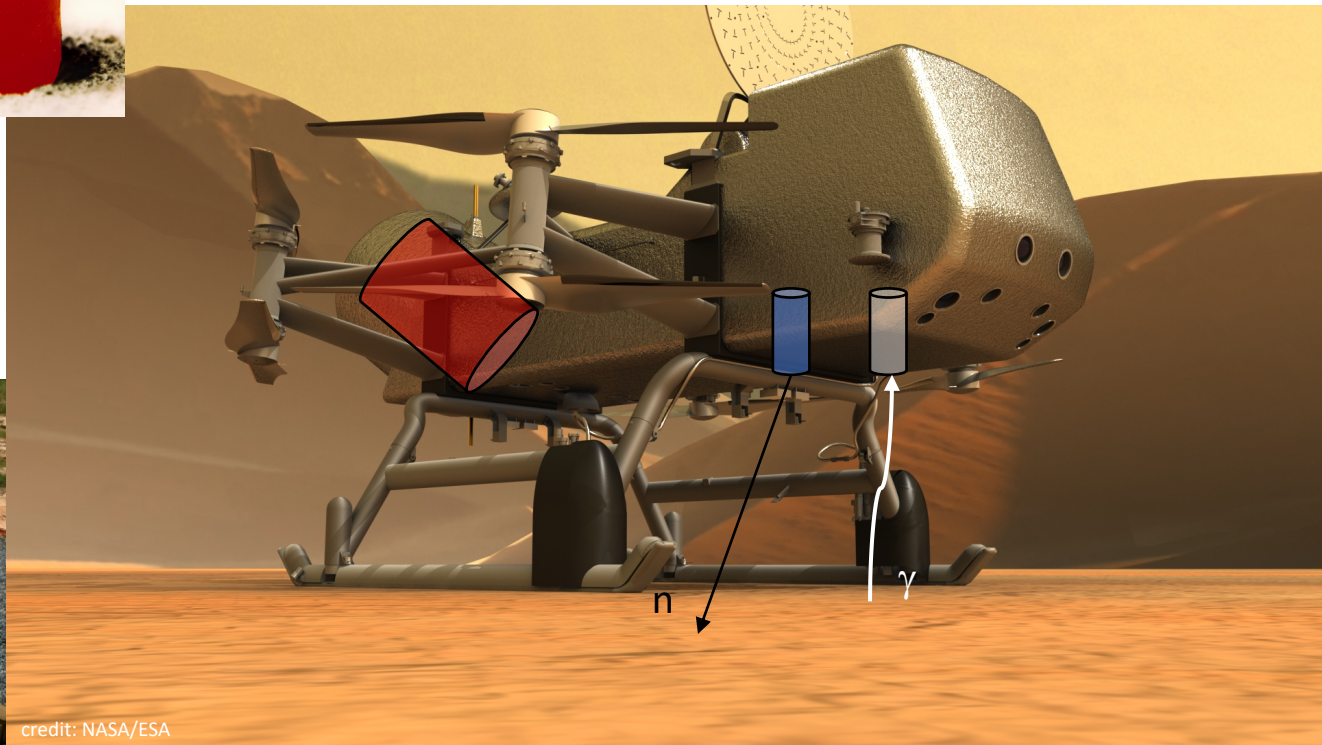
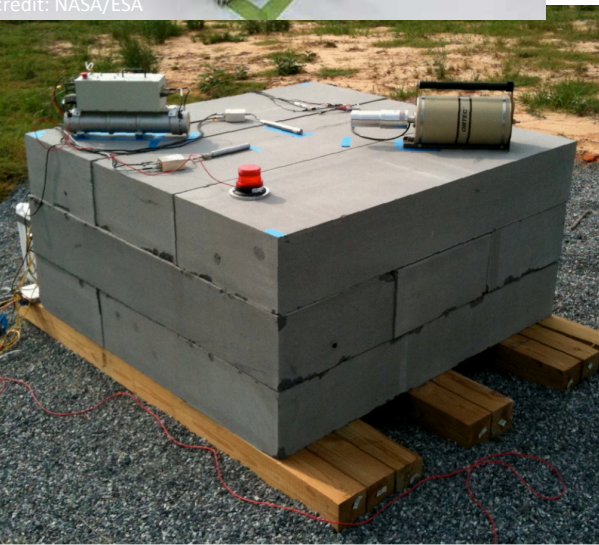








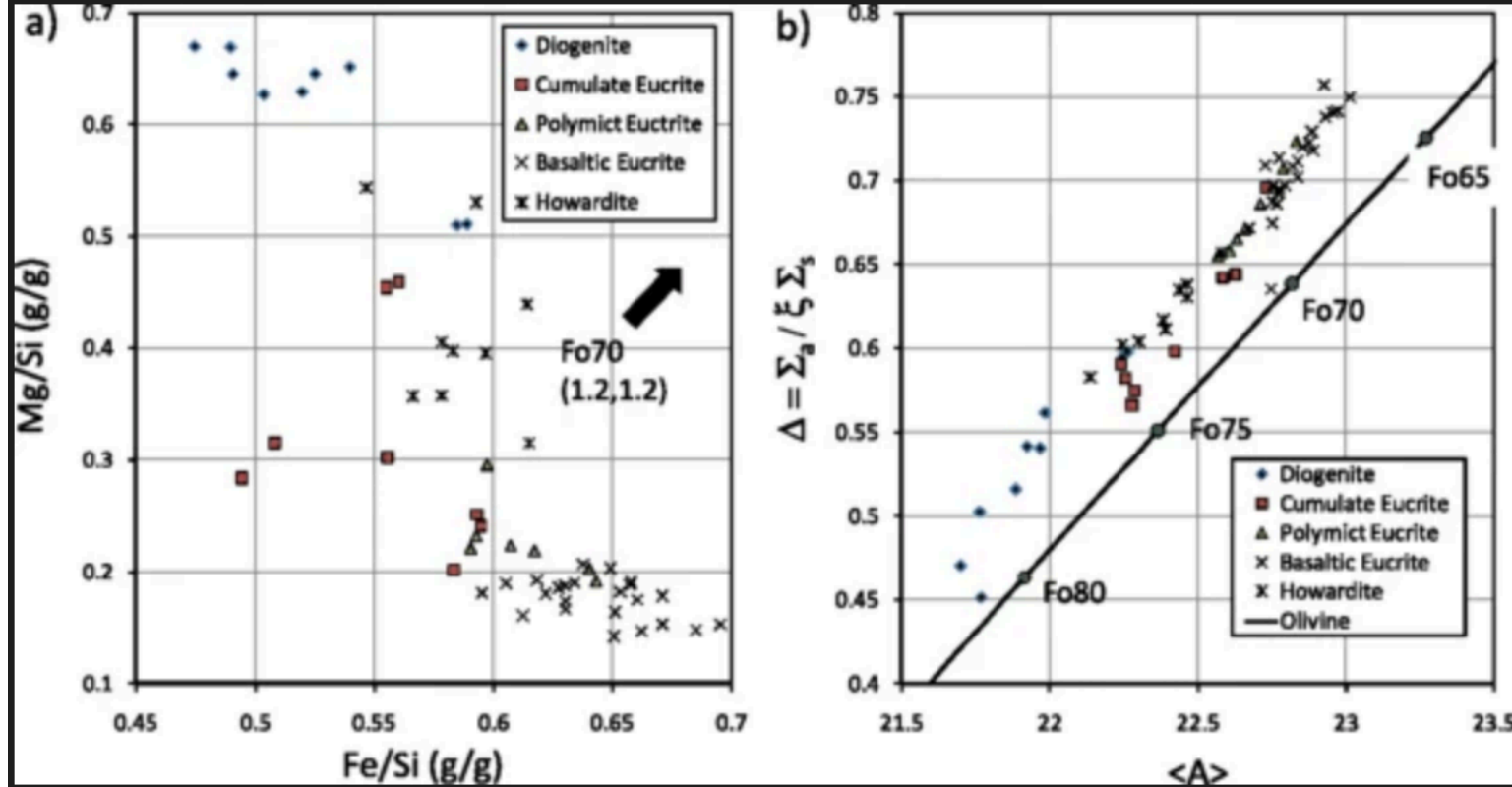
credit: NASA/ESA



credit: NASA/ESA

A detailed digital illustration of a lunar or planetary surface. The foreground is filled with numerous grey and brown rocks of various sizes, some with sharp edges and others more rounded. The ground is a mix of light and dark patches, suggesting different mineral compositions. In the middle ground, the terrain levels out slightly before meeting a large, dark, and heavily cratered planet that dominates the right side of the frame. The planet's surface is textured with intricate details of craters and ridges. In the upper left corner, a bright, glowing sun or star is visible, casting a strong light across the scene and creating a lens flare effect. The sky is a deep, dark blue-black, filled with numerous small, distant stars.

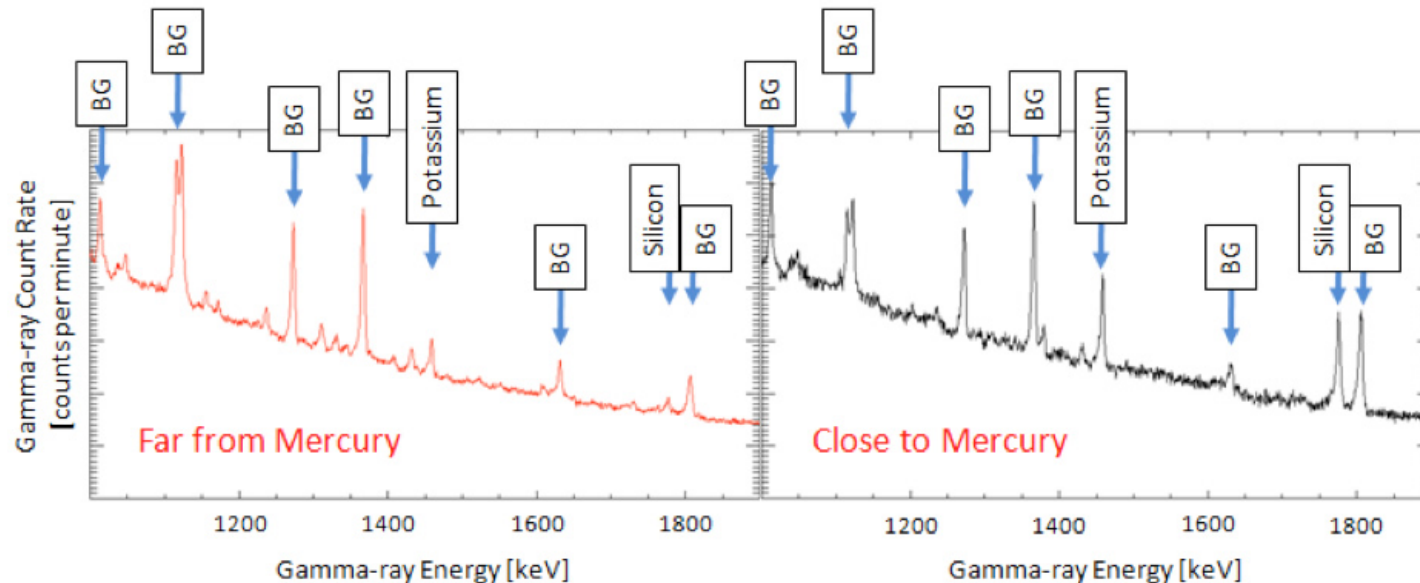
Thank you



A scatter plot of elemental ratios Mg/Si and Fe/Si discriminates HED whole rock types and olivine. Ratios determined from whole-rock HED compositions are plotted. Olivine with 71% molar forsterite (Fo71) is the average composition of olivine in diogenites and is thought to be representative of Vesta's mantle.

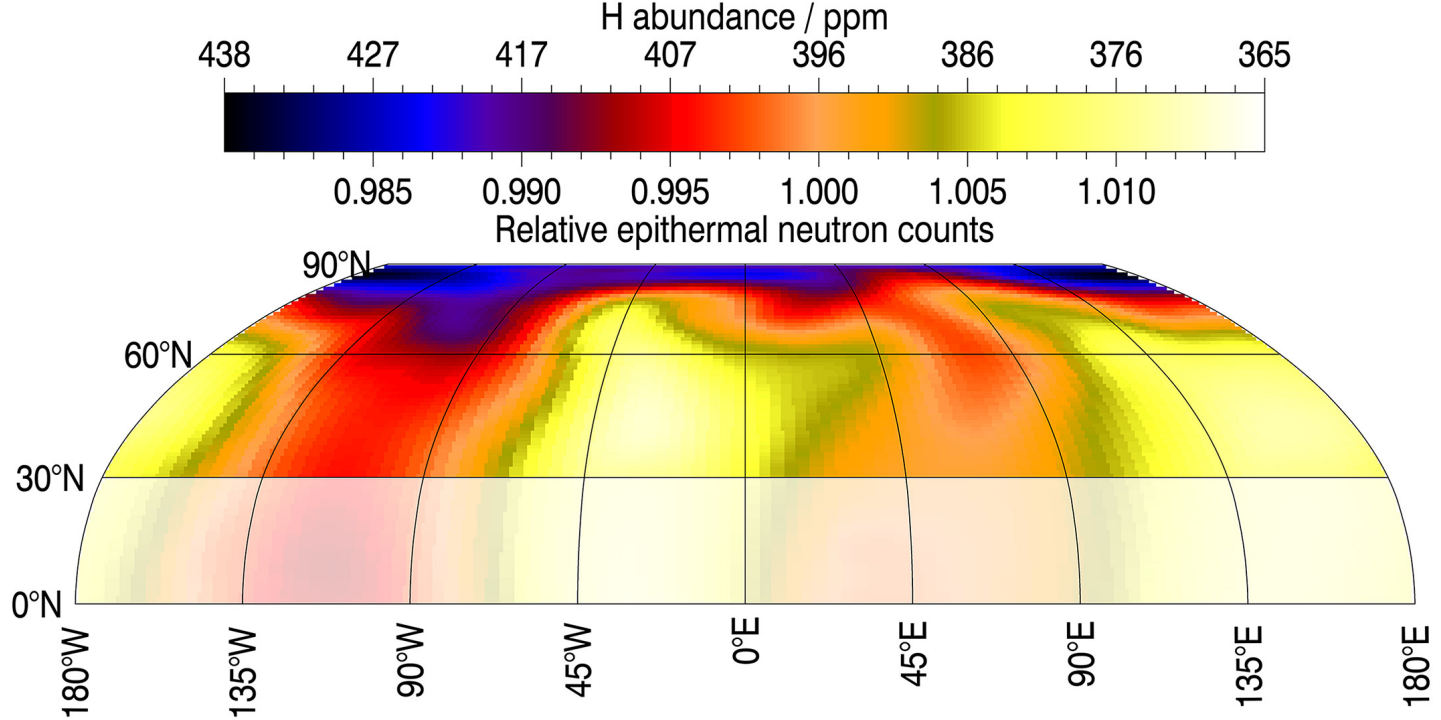
(b) Similarly parameters determined by neutron spectroscopy Δ and $\langle A \rangle$ are sensitive to HED whole-rock types and variations in olivine composition

21 MESSENGER

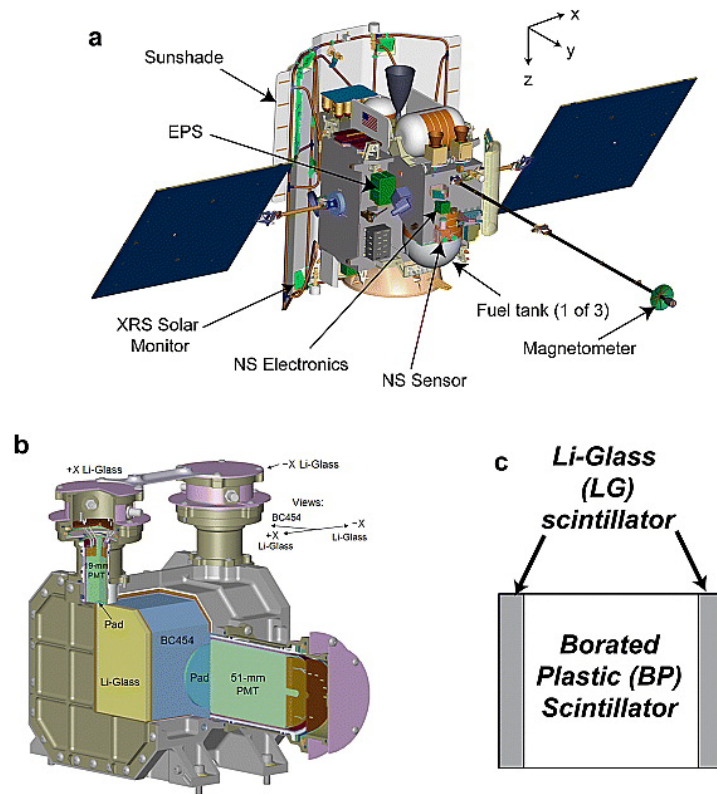


Two example gamma-ray spectra acquired by the MESSENGER Gamma-Ray Spectrometer, with gamma-ray count rates shown as a function of energy (keV, or kilo-electron volt, is a unit of energy). To the left is shown a gamma-ray spectrum collected while MESSENGER was far from the planet; to the right is a spectrum obtained close to the surface (less than 2000 km altitude). “BG” denotes background gamma-ray peaks. Two particular gamma rays, at 1460-keV resulting from potassium and at 1779-keV resulting from silicon, are highlighted, as they show clear enhancements near the surface. These data demonstrate the presence of potassium and silicon on Mercury's surface. Other unlabeled peaks in the gamma-ray spectra in this





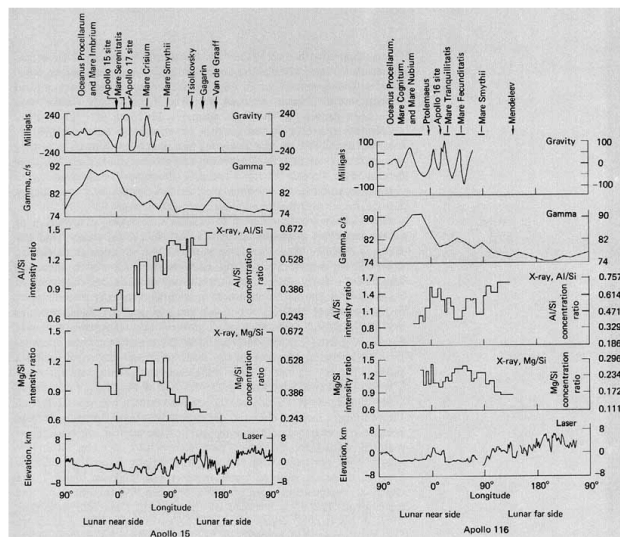
At the resolution of the MESSENGER neutron measurements, the footprint-averaged increase in hydrogen seen at the north pole is ~ 75 ppm, which is consistent with earlier work showing a 50- to 100-ppm H increase at high latitudes (Lawrence et al., [2013](#)). Using both epithermal and fast neutron data, this earlier result was shown to be consistent with the radar-bright regions containing a hydrogen-rich layer buried beneath a desiccated layer 10–30 cm deep. In the midlatitudes, the hydrogen abundance appears to vary periodically with wavelength of 180° in the longitudinal direction. It is interesting to note that maximum and mean surface and near-subsurface temperatures on Mercury also vary with latitude due to its 3:2 spin-orbit resonance. This resonance leads to the presence of hot poles (at 0°E and 180°E) that always experience noon at perihelion and cold poles (at 90°E and 270°E) that experience noon at aphelion (Vasavada et al., [1999](#)). The hydrogen lows of ~ 365 ppm are approximately coincident with the hot poles, and the highs (~ 400 ppm) are approximately collocated with the cold poles. A hydrogen correlation with mean or maximum temperature might be explained as a thermal stability/mobility effect, the result of implantation differences, or as the effect of mineralogy.



2 ^6Li glass scintillators on the ends separated by a beveled cube of neutron-absorbing, borated plastic scintillator. The glass scintillator plates are loaded with lithium enriched in ^6Li to detect thermal and epithermal neutrons. The borated-plastic central scintillator counts epithermal neutrons from all directions and measures the energy depositions of fast neutrons. All three scintillators are viewed by individual PMTs.

(a) Engineering drawing of the MESSENGER spacecraft [Leary et al., 2007] showing the locations of the Neutron Spectrometer (NS sensor), X-Ray Spectrometer (XRS) solar monitor, Magnetometer, and Energetic Particle Spectrometer (EPS) sensor relative to the sunshade at left and the three intervening fuel tanks that shield the NS from the Sun. (b) Engineering drawing of the MESSENGER NS and a simplified schematic of the placement of the three NS sensor components. BC454 in Figure 1b refers to the designation of (c) the borated plastic scintillator.

Apollo



[25] FIGURE 15 [above]. - Curves showing correlations of some physical and chemical properties recorded by elected remote sensing instruments carried in the SIM bay with topographic and geologic features. Left: Representative sensing curves plotted from data recorded along some of the Apollo 15 ground tracks. Right: The same types of data but along some of the Apollo 16 ground tracks. For purposes of location, selected geographic features are shown at the top of the graphs and degrees of longitude along the bottom. These curves show many interesting relations including (1) the positive gravity anomalies (concentrations of mass or "mascons") marking the circular mare basins, (2) the high gamma radiation from the border between Oceanus Procellarum and Mare Imbrium, (3) the inverse relationship between ratios of Al/Si and Mg/Si, (4) the systematic change in these ratios from maria to terrae, and (5) the differences in elevation between mare areas (low) and terra areas (high). Another significant observation is that the east limb of the Moon near Mare Smythii is much lower in elevation than other areas along the Apollo 15 and 16 ground tracks. In fact, the mare areas on the front side decrease in elevation from the west limb at Oceanus Procellarum to the east limb at Mare Smythii.

[26]...impact basins with mare filling are Imbrium, Crisium, and Orientale. Other multiringed circular basins of probable impact origin are, however, devoid or nearly devoid of mare fill. Structural, geochemical, and topographic differences between the circular and irregular mare areas have been proven by the laser altimeter, lunar sounder, gamma ray spectrometer, and X-ray fluorescence experiments, as well as by photointerpretation. The circular maria are bounded by striking cliff-forming arcuate segments of crustal blocks while the irregular maria have low serrate edges. Positive gravity anomalies ("mascons") delineated by the S-band transponder experiment are associated with the impact basins but are absent over the irregular areas.

There are many hypotheses to explain the varying distribution of crustal materials documented by the Apollo orbital sensors and the samples returned from the lunar surface. The variation in thickness, composition, and elevation of the mare and terra regions, the increased gamma ray activity observed in the midfront and far sides, the increased magnetic and gamma ray measurements obtained over some limb areas, and the essential differences between irregular and circular mare basins and the highland areas all imply a controlling mechanism. A theory based on mantle convection (the internal circulation of hot material) gives a possible explanation for the observed sensor data and describes a possible controlling mechanism for the chemical, geophysical, and topographic variations. Very early in the history of the Moon's formation, when it was very hot and fluid, the mantle material was separated from the primordial melt by chemical differentiation. Lower density material became concentrated in the upper part of the mantle, whereas denser material settled in the lower part. Convection currents within the mantle then partially stripped the lighter weight material from some areas to cause the marked variation in crustal thickness, density, and chemical composition now observed between the present terra and mare areas. The areas stripped of lighter weight material were then flooded by basalts, which presently lie on a greatly thinned crust. Localized areas of increased concentrations in gamma ray and magnetic activity were caused by internal circulation and concentration of materials with higher magnetic and gamma ray properties. The mantle convection theory, however, is still being debated. True understanding of the development of the lunar crust may require years of additional study.

The mechanics of impact cratering have been studied intensively with the aid of the Apollo data. Craters ranging in size from the giant basins hundreds of kilometers across (like the Imbrium basin), to the smallest craters visible in orbital photographs (1 m in diameter), to microcraters on the surface of minute glass spheres contained in the returned lunar soil samples have been studied.

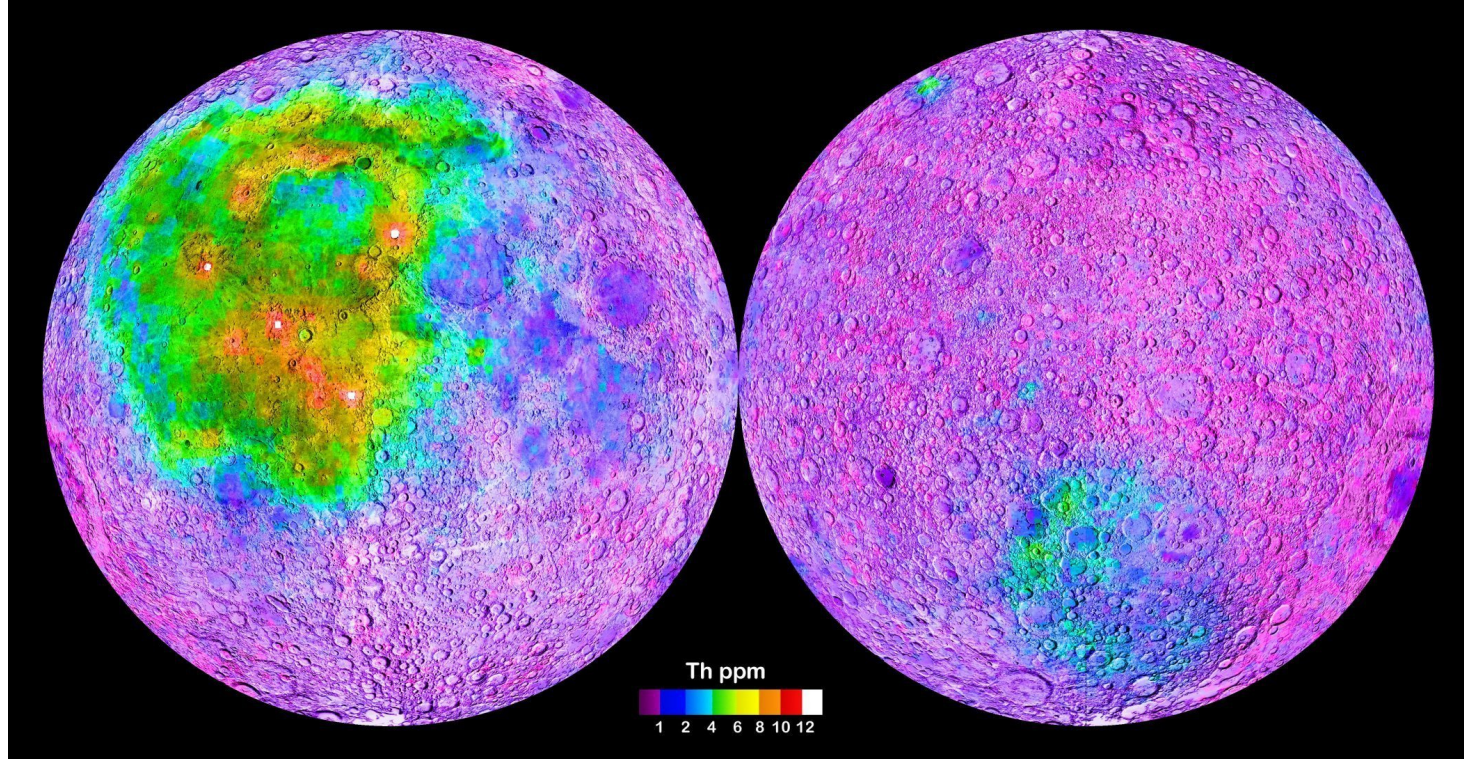
Crater ejecta material has been studied and classified into two groups: ballistic ejecta that is thrown out to form linear or curved patterns of rays and clusters of secondary craters on the Moon's surface, and fine-grained fluidized ejecta that locally blankets the lunar surface and forms patterned flows extending downrange from the primary [27] impact crater. The continuous ejecta blanket is apparently replaced by base surge flow on the surface surrounding the crater. A striking example of surface patterns created by ejecta flow and its interaction with the local topography is found near the far-side crater King (fig. 159).

The continued bombardment of the lunar surface by meteoroids and secondary impact material has formed a regolith on the surface composed of breccia fragments and unconsolidated fragmental debris. The thickness and age of the regolith vary systematically. In general, thickness estimates based on crater shape agree well with estimates based on bistatic radar measurements.

A variety of features has been investigated and recognized as being of volcanic origin. Other terrain features have been more equivocally classified as possibly volcanic in origin. A succession of lava flows has been mapped in the Imbrium basin. Dark halo craters have been studied extensively and divided into two classes: The round, smooth-sided craters with no visible blocks in the crater walls are believed to be volcanic, and the dark halo material is thought to be composed of very fine-grained volcanic ejecta. Dark halo craters having irregular outlines may be impact craters from which darker material was exhumed at the time of impact. Lines or chains of craters have also been classified into two groups: volcanic crater chains (Hyginus Rille and Davy crater chain) and secondary impact crater chains extending radially from large craters (such as Copernicus, Kepler, and Aristarchus) and formed by ballistic ejecta from the large craters.



Lunar Prospector



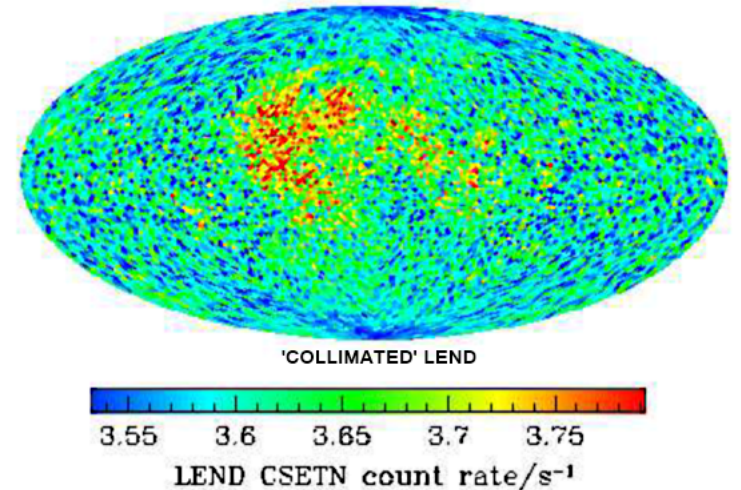
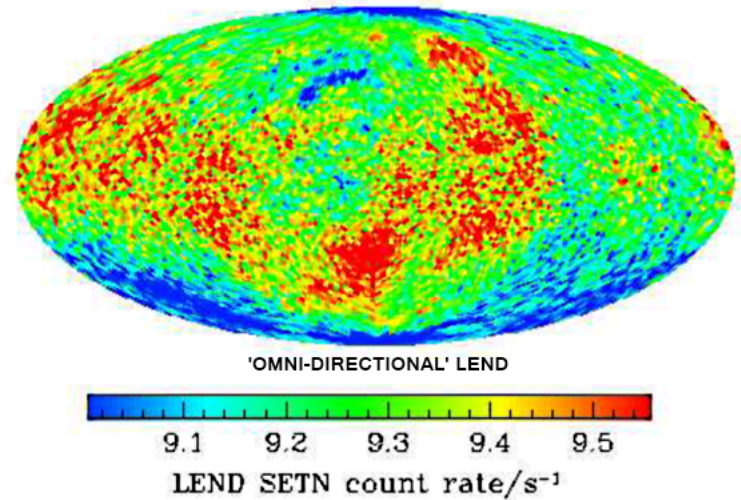
Thorium map of the Moon A map of the thorium content of the lunar surface based on Lunar Prospector data shows that a large area on the nearside of the Moon, including the Imbrium basin and Oceanus Procellarum, is enriched in thorium relative to the rest of the Moon. There is also an area of enriched thorium on the farside, within the South Pole-Aitken Basin, but it is less enriched than the area on the nearside. *Data: NASA / ARC / Jeff Gillis; map by Paul Spudis*

16 Lunar Reconnaissance Orbiter

A scientific dispute...

Over the last year, the [LEND team's reports](#) have appeared in the scientific literature. To the surprise of most lunar scientists, their team claimed that in all but two or three isolated cases, hydrogen detected by LEND does not correlate with the polar dark areas. This puzzling result would seem to indicate that perhaps we do not fully understand the nature of the polar hydrogen and the processes involved in their creation and retention.

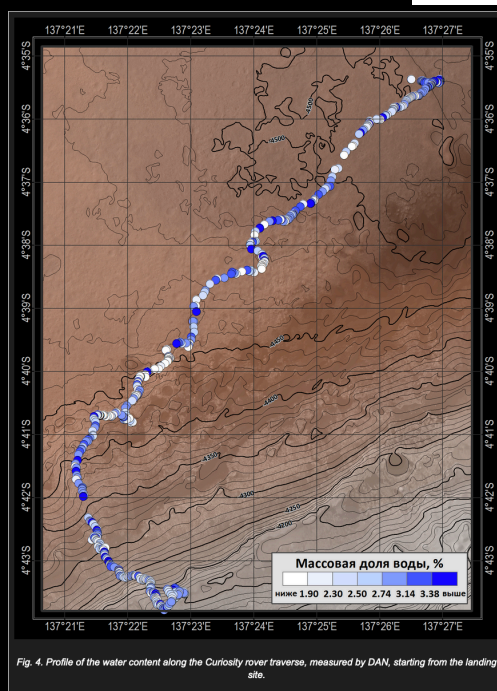
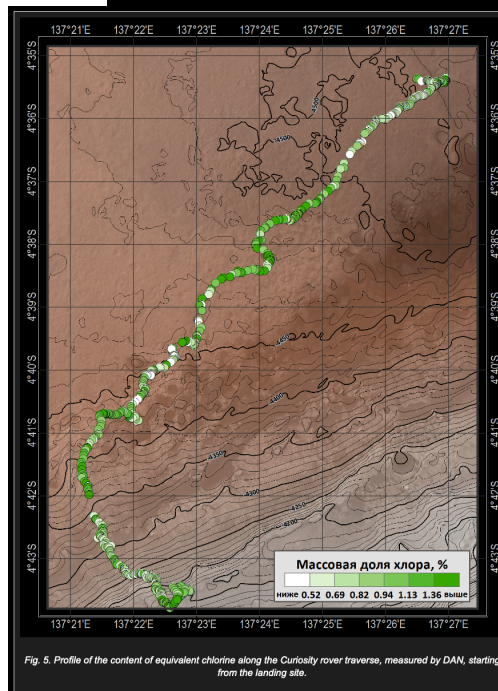
Several scientists (I will collectively call them the “skeptics”) who work with neutron data from LP and other missions, differed with the LEND team conclusions, who in turn vigorously defended their results as valid, citing as evidence the coincidence of laser altimetry and neutron data over one crater (Shoemaker) near the south pole of the Moon. Having studied the LEND data set themselves, the skeptics contended that the actual average count rate for neutrons is less than half of that quoted by the LEND team, meaning that the hydrogen content inferred from the LEND data are significantly less precise than claimed. Moreover, they estimate that the signal from the collimated (high resolution) detectors is only a few percent of the total signal, whereas the LEND team claims that it is roughly one-third of the total. The skeptics make the point that if the collimator is working as the LEND team claim, the map derived from the collimated detector should be a sharper, higher resolution version of the low-resolution map made in the uncollimated mode. In fact, the skeptics contend that the two maps look completely different (see figure at top of this post), suggesting that the collimated product is detecting something else; based on the observed pattern, it is probably related to the amount of iron in the lunar surface.



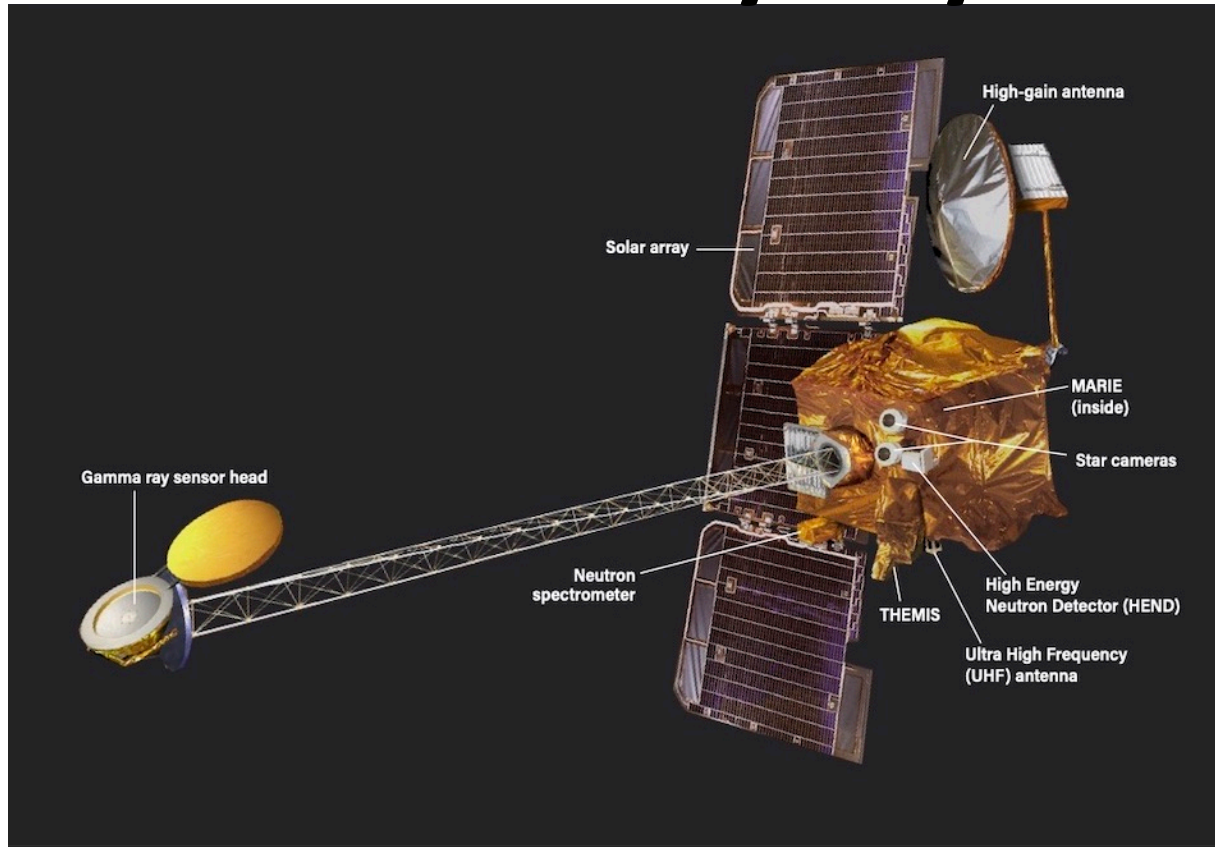
Curiosity

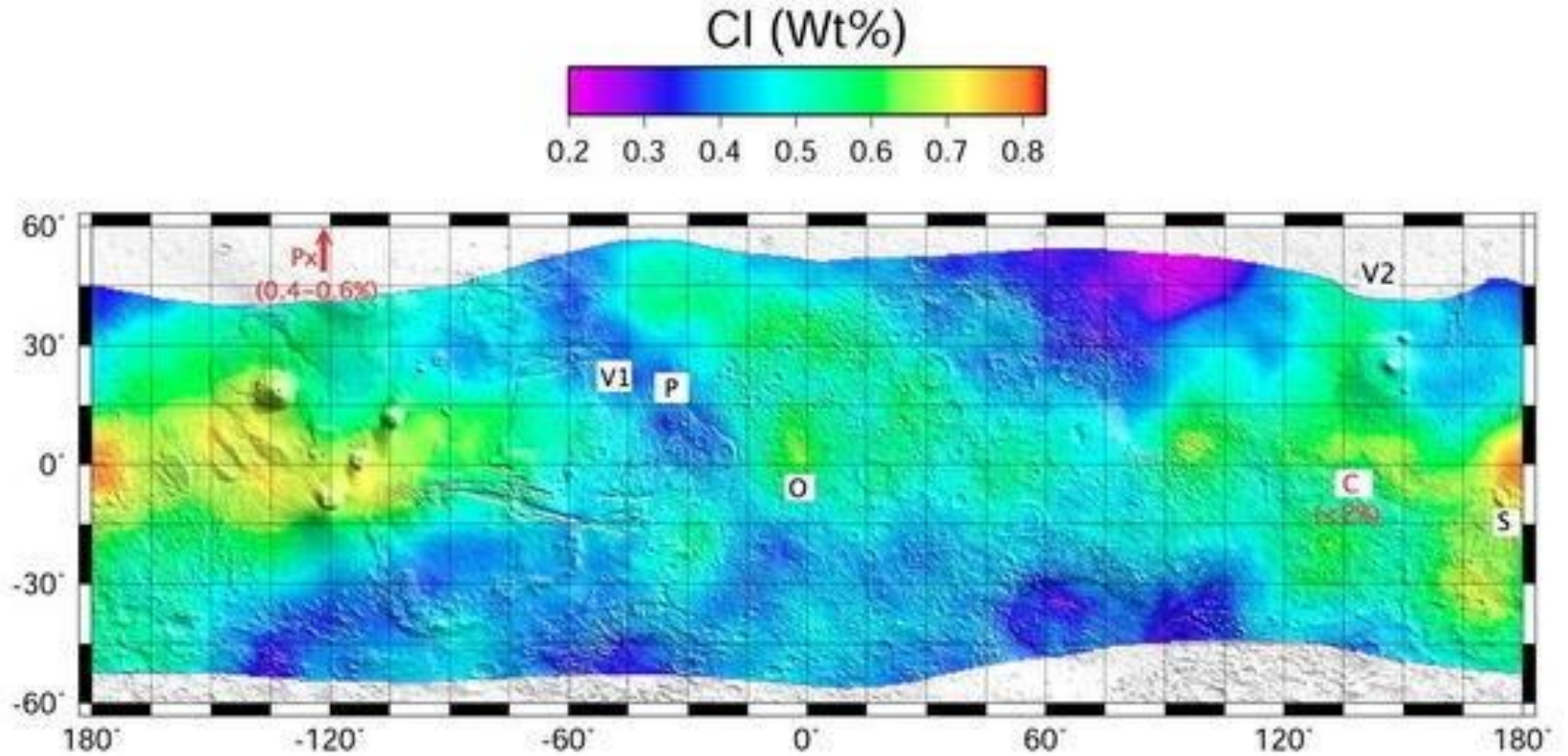
DAN

Below are main scientific results of the DAN instrument during its operation onboard the NASA Curiosity rover. The profiles of the content of subsurface water and neutron absorbers (primarily such common chemical elements as chlorine and ferrum) measured by the DAN instrument are shown. The neutron absorber profile is represented as an equivalent chlorine content, as an element whose spatial variability makes the main contribution to the variations observed in the DAN data. The average content of bound water along the rover traverse is about 2.5%, and chlorine about 1% by mass fraction. DAN has been working on the surface of Mars for more than 6.5 years (more than 2,400 Martian days or sols), and the rover traversed more than 20 km away from the landing site. Each year, DAN performs approximately 700 measurements in the passive mode and 120 measurements in the active mode (using the neutron generator). About 1,300,000 neutron pulses of the neutron generator are spent on this. In addition, each year 650 instrument control shifts are performed (daily work), of which approximately 75% is provided by the staff of the IKI RAS



Mars Odyssey

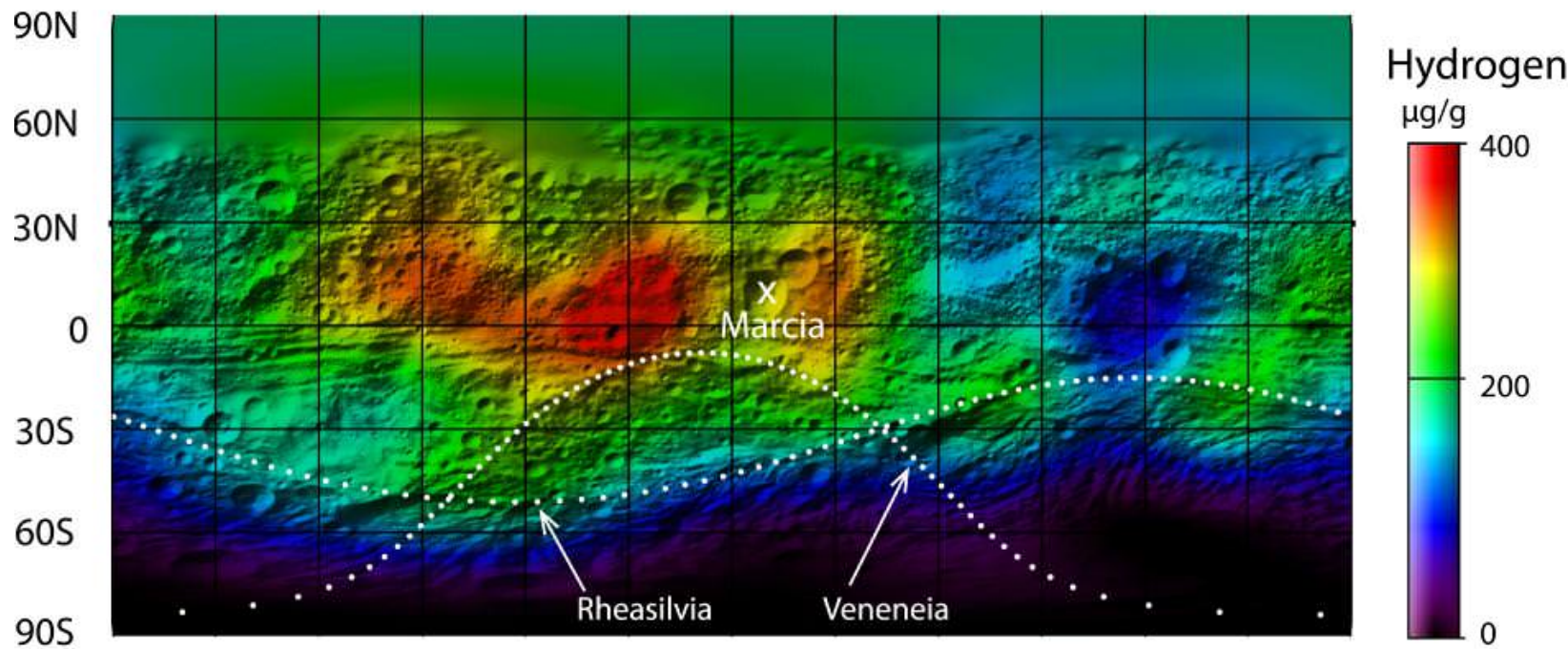




Equatorial and midlatitude distribution of chlorine (Cl) within the top one meter of Mars measured by the Gamma Ray Spectrometer onboard NASA's Mars Odyssey. The global concentration of Cl is similar to the measured concentration of ClO_4^- at two landing

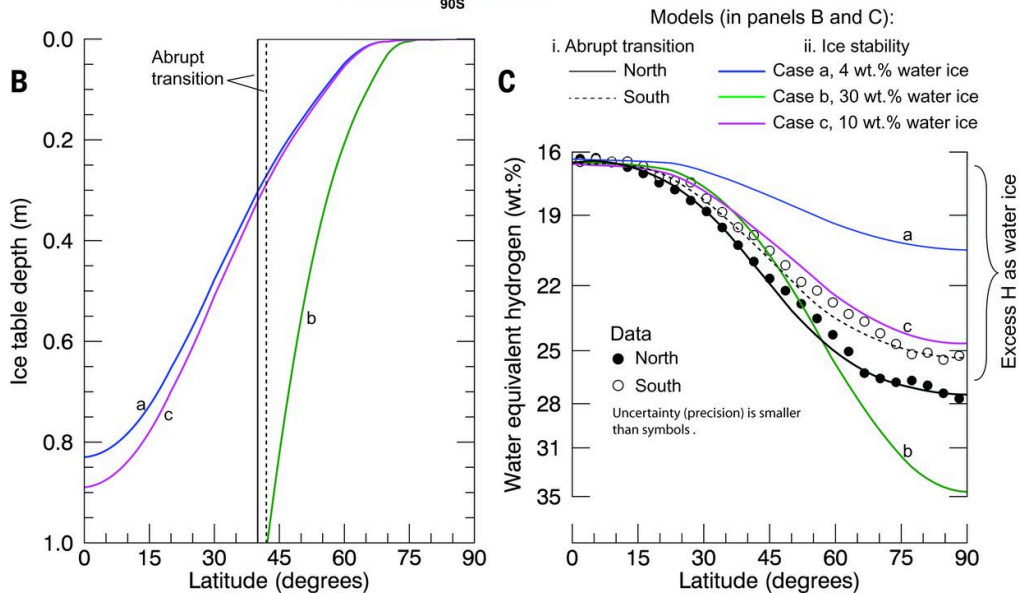
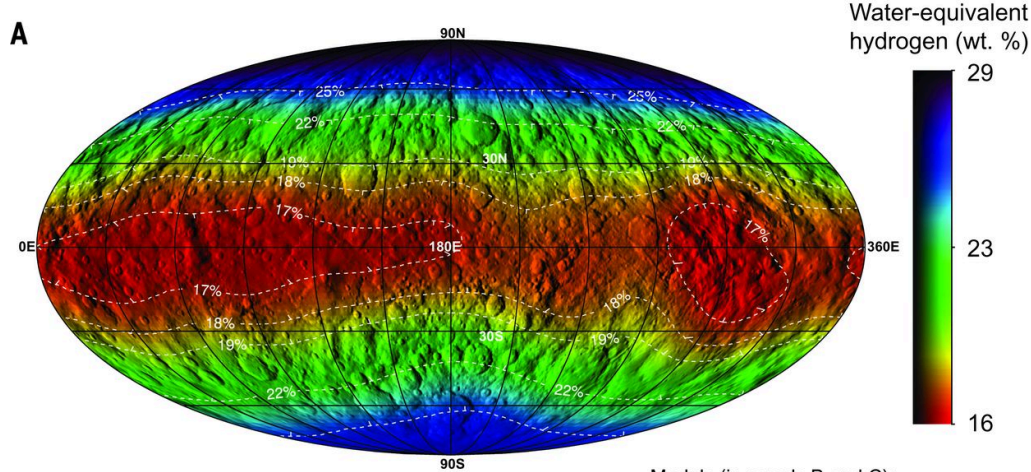


DAWN



The source of the hydrogen within Vesta's surface appears to be hydrated minerals delivered by carbon-rich space rocks that collided with Vesta at speeds slow enough to preserve their volatile content



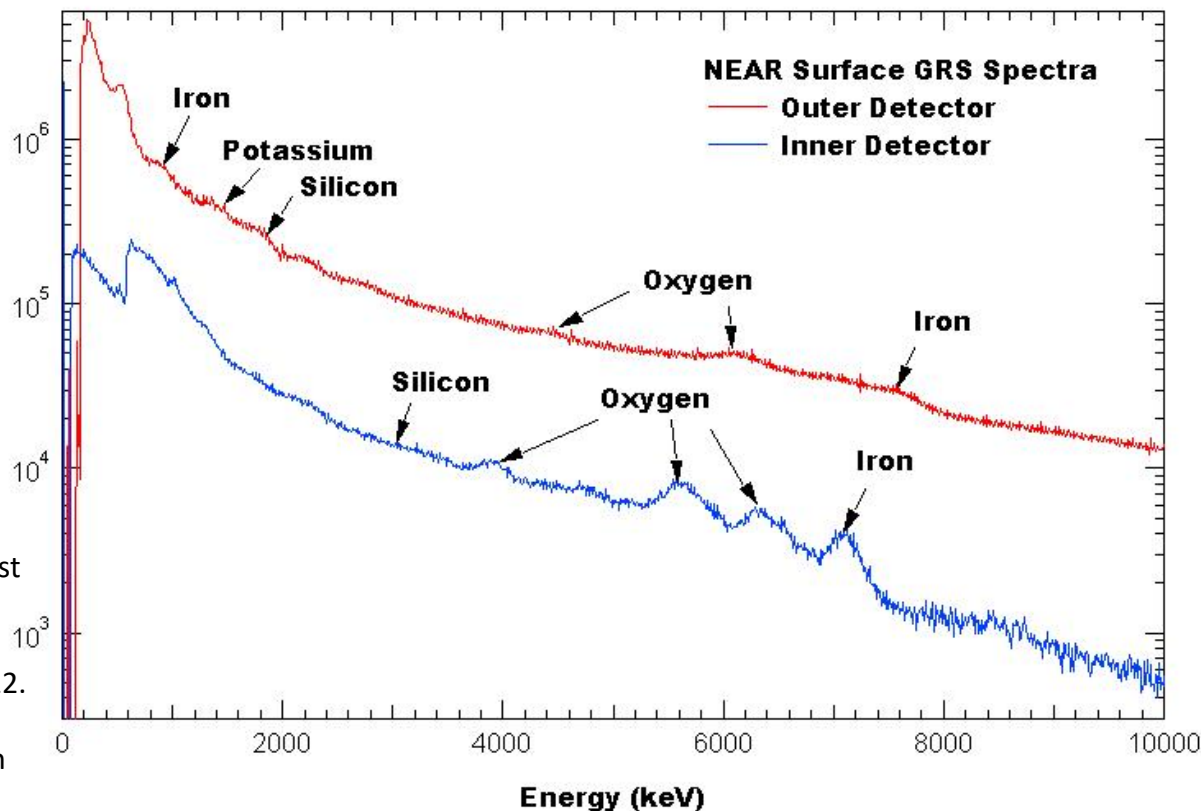


The dwarf planet Ceres in the inner solar system is thought to have a crust made of a mixture of rock and ice. Prettyman *et al.* used neutron and gamma-ray spectroscopy from the Dawn spacecraft to peer below Ceres' surface and map the subsurface composition. They found evidence for water ice across the dwarf planet, with water making up a larger fraction of the material near the poles than around the equator.

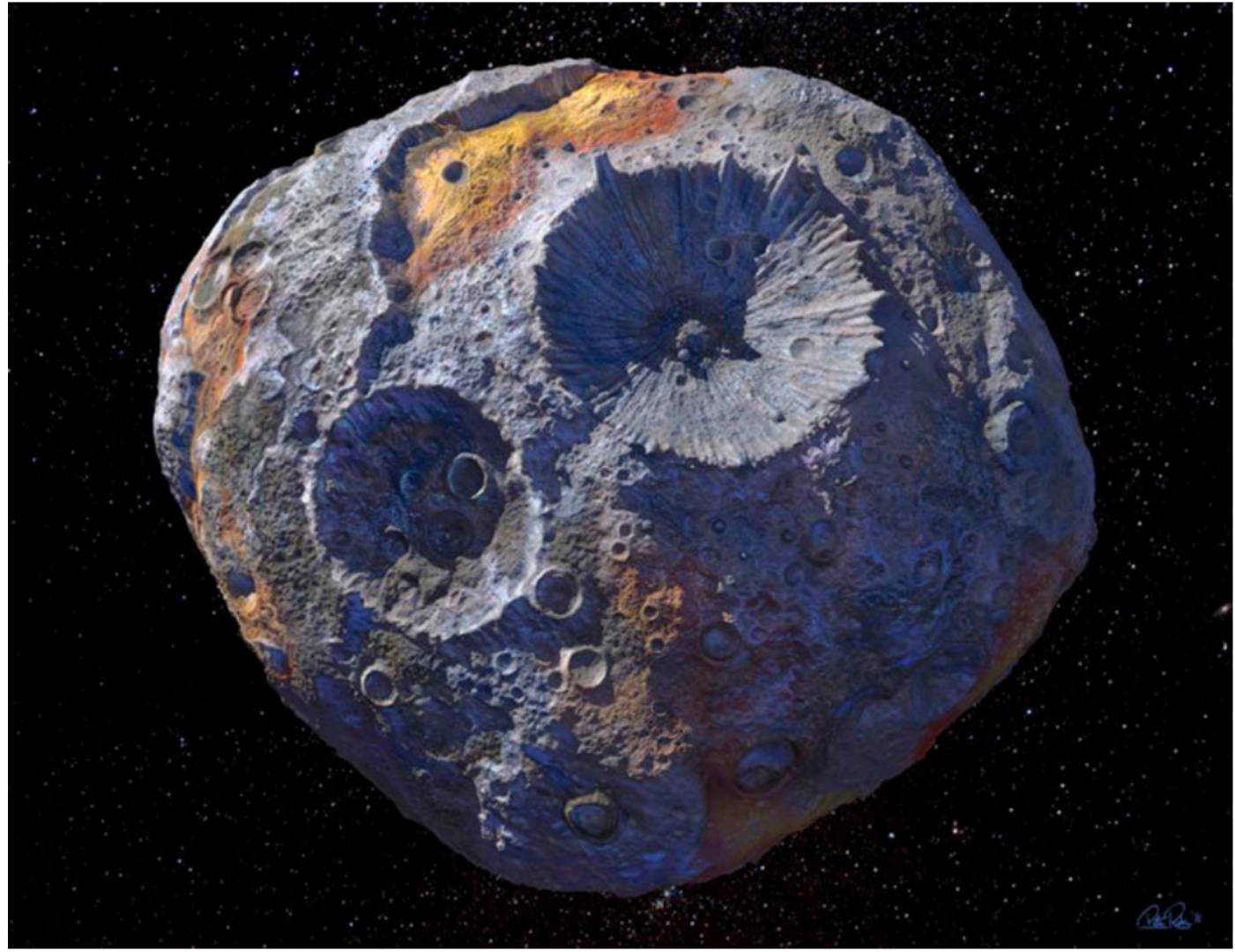
NEAR Shoemaker

This chart shows the gamma-ray spectrum from the surface of Eros. These scientific data -- the first ever collected on the surface of an asteroid -- result from 7 days of measurements following NEAR Shoemaker's historic landing on February 12. The gamma-ray instrument has two detectors -- marked above by the red and blue traces -- which picked up clear signatures of key elements in the composition of Eros. These data, which surpass in quality all the data accumulated by this instrument from orbit, will help NEAR scientists relate the composition of Eros to that of meteorites that fall to Earth.

Relative Intensity



Psyche



The Psyche mission is a journey to a unique metal asteroid orbiting the Sun between Mars and Jupiter. What makes the asteroid Psyche unique is that it appears to be the exposed nickel-iron core of an early planet, one of the building blocks of our solar system. Deep within rocky, terrestrial planets - including Earth - scientists infer the presence of metallic cores, but these lie unreachably far below the planets' rocky mantles and crusts. Because we cannot see or measure Earth's core directly, Psyche offers a unique window into the violent history of collisions and accretion that created terrestrial planets.

Science Goals

Understand a previously unexplored building block of planet formation: iron cores.

Look inside terrestrial planets, including Earth, by directly examining the interior of a differentiated body, which otherwise could not be seen.

Explore a new type of world. For the first time, examine a world made not of rock and ice, but metal.

Science Objectives

Determine whether Psyche is a core, or if it is unmelted material.

Determine the relative ages of regions of Psyche's surface.

Determine whether small metal bodies incorporate the same light elements as are expected in the Earth's high-pressure core.

Determine whether Psyche was formed under conditions more oxidizing or more reducing than Earth's core.

Characterize Psyche's topography.



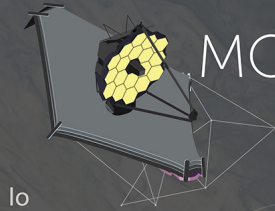
radioisotope thermoelectric generator (RTG)

The process starts when researchers at Idaho National Lab send neptunium-237, itself a radioactive metallic oxide, to Tennessee, where automated machines press it into pellets the size of pencil erasers. Next, 52 of these pellets are stacked into metal rods called targets and placed in a nuclear reactor at either Oak Ridge or Idaho National Lab, where they are bombarded with neutrons to produce plutonium. After it's left to cool for a few months, the plutonium is shipped to Los Alamos National Laboratory in New Mexico, where another machine presses the small plutonium pellets to form larger ones the size of marshmallows. Then they're ensconced in a casing made out of iridium, a virtually indestructible metal that would prevent radioactive contamination in case of an accident when the rover is launched. Finally, the armored plutonium is shipped to Idaho National Lab, where 32 pellets are loaded into the rover's nuclear battery before it's installed on the vehicle.

Perseverance: The RTG is designed to produce about 110 watts of electrical power to begin the mission. The system has a design life of 17 years, but it can be expected to produce power much longer than that. the Perseverance rover uses ~ 5 kilograms of plutonium.



MOONS: ACTIVE WORLDS



Io

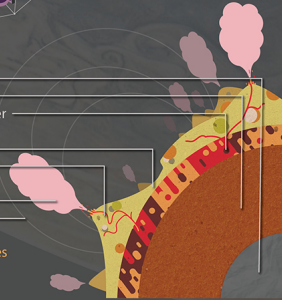
1132 mi (1822 km) radius

Iron core
Rocky mantle
Global subsurface magma layer

Silicate surface
Volcanoes

Sulfur plumes
Induced magnetosphere

More than 400 active volcanoes



Europa

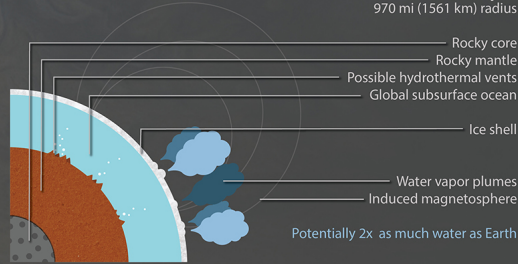
970 mi (1561 km) radius

Rocky core
Rocky mantle
Possible hydrothermal vents
Global subsurface ocean

Ice shell

Water vapor plumes
Induced magnetosphere

Potentially 2x as much water as Earth



Enceladus

157 mi (252 km) radius

Rocky, porous core
Hydrothermal vents
Global subsurface ocean

Thick ice shell

Plumes of water vapor and ice particles

Tiny particles of ice are ejected at ~800 mph



Titan

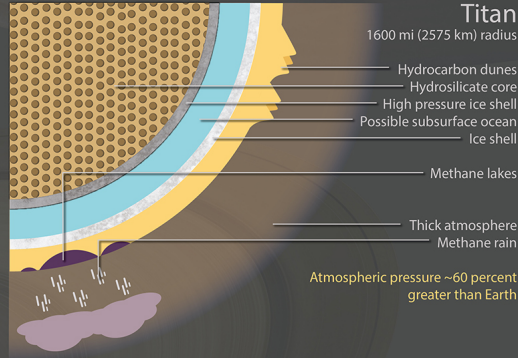
1600 mi (2575 km) radius

Hydrocarbon dunes
Hydrosilicate core
High pressure ice shell
Possible subsurface ocean
Ice shell

Methane lakes

Thick atmosphere
Methane rain

Atmospheric pressure ~60 percent greater than Earth



Moons and features not to scale

